Resistance Spot Mash Welding of Cu Wires for Electric Car Batteries and Motors

Warren Peterson*, Jerry Gould*, John Agapiou**, Thomas A. Perry**, James G. Schroth**
***Edison Welding Institute**
****GM Manufacturing Systems Research**

Abstract

Joining high current carrying copper wires and leads for electric batteries and motors can be accomplished using either arc or resistance welding methods. Resistance methods have the advantage of faster cycle times but traditionally have been difficult to welds since the wires are generally made from commercially pure copper. The goal of this work was to examine resistance mash welding (RMW) to join commercially pure wire of relatively large cross sections (3.44 × 3.66 mm). Using the traditional RMW process, the joint area is heated under load to simultaneously soften and forge the metal at the wire-to-wire (faying) interface. In this program, a separate forge force is applied to increase the local interfacial strain. Forging the joint at elevated temperature causes thinning/adsorption of copper oxides, exposing nascent copper in the formation of a strong solid state joint. The RMW weld cycle, as used in this program, was broken into several distinct phases (pre-heat, weld, and forge) with independent starting and ending currents, electrode pressures, and durations. Both cross- and parallel-wire weld joint arrangements were evaluated in this study. Modifications to the fast-follow-up head were used to maintain contact between the electrodes and the work and to enable forging of the joint. Excellent quality copper-to-copper joints were produced in this program using the best practice parameters. Weld strengths for the cross-wire joint geometry were nominally greater than 1.56 kN (350 lb) and the strength of the parallel-wire joint geometry were nominally greater than 670 N (150 lb). An optimum joint thickness was shown to be a critical indicator of joint strength since the upper bounds for strength were related to the critical forging strain and thinning of wire. Optimum weld times produced welds of acceptable strength and consistency.

Introduction

Traction motors are largely designed around “bar-wound” stators which incorporate large-cross-section rectangular copper wires to maximize the conductive metal area within the motor stator channels. Individual pieces of copper wire are bent into “hairpin” shapes and inserted into stator lamination stacks. These hairpins must be joined together to create the required electrical circuit.[1] Joining of copper can be complicated by its very high thermal conductivity, making it difficult to concentrate sufficient energy at the joint position to produce fusion without overheating adjacent areas.

Gas tungsten arc (GTA) welding has been used to join the stator wires, as illustrated in Figure 1. This process provides an adequate joint for oxygen-free, high-conductivity (OFHC) copper, but oxygen-containing tough pitch copper have tended to exhibit porosity associated with the combination of hydrogen (in the arc) and oxygen (in the substrate) to produce water vapor at the joint.[2] Alternate processes for joining copper are needed that offer improved process robustness, reproducibility, joint durability, and decreased degradation of adjacent wire insulation systems. Consequently, resistance mash welding (RMW) was evaluated in this study of simulated bar wound magnet wire joint specimens. In this application of RMW, a multistep force and current regiment is used to manage the temperature and deformation of the wires during the joining process. Initially, the joint area is heated under a relatively low load, so that the parent metal becomes sufficiently soft to enable significant deformation of the joint interface. The electrode force is subsequently rapidly increased to produce local strain at the wire-to-wire (faying) interface, this causes surface oxides to fracture and expose nascent copper so that metallurgically clean copper surfaces are brought into contact at elevated temperature to form a strong joint.[3] While a good copper-to-copper bond between two wires can be achieved through application of pressure and current with a conventional spot welding machine, managing the dynamic response of the welding electrodes is critical, as will be shown in this paper.

In order to achieve a strong, low resistance, clean copper-to-copper joint, the process parameters must be optimized to insure significant solid-state joining without overheating the copper and expelling it or causing it to stick to the electrode faces. The use of the fast followup head was an important aspect of this study. The purpose of this work was to define a recommended weld schedule for the cross- and parallel-wire joint geometries. In addition, several sources of joint strength variations associated with equipment, geometry, and schedule were investigated. This paper details experiments aimed at achieving high-quality copper-to-copper joints with a minimum of time, energy, and applied force.

Methodology

Figure 2 shows a schematic diagram of possible current and force variations with time for the RMW process. Critical elements of the RMW process are to focus the heat input at the faying interface and minimize heating of the copper-electrode interfaces. Resistance heating occurs when current flow from the spot welding gun into the base metal, across the faying interface, into the second piece of base metal, and back to ground through the remainder of the gun structure. I^2R heating occurs in each element of the path and at every interface due to contact resistance.

Several process variables influence the peak temperatures generated by the process:

1. Electrode geometry
2. Electrode surface texture
3. Electrode cooling
4. Copper surface preparation (surface texture)
5. Copper resistivity

The texture and geometry of the electrode face are important to minimize contact resistance at the copper-to-electrode interfaces. A surface with too smooth a profile may fail to breech native oxides and cause high resistance. Alternately; asperity contact may dominate an electrode with too rough of a profile, limiting the conductive area and producing excessive resistive heating. The work done in this study was based on RWMA Class 20 electrodes, which has acceptable anti-sticking qualities.

Most heavy-duty spot welders have water cooled electrodes, but the fast follow-up attachment, used here, did not include electrode cooling. For these experiments, external flood coolant was applied to the weld gun and captured in a bucket below.

In addition to these variables, the weld cycle can be broken up into several distinct phases that can be thought of as pre-heat, weld, and forge. Each of these phases may have independent starting and ending currents (a linear ramp), independent electrode pressure, and a programmable duration.

Two types of weld joints, cross- and parallel-wire arrangements shown in Figures 3 and 4, were investigated in this study. The first joint uses the contact area between two intersecting wires, cross-wire joint, to concentrate weld current and produce metal displacement. Large-diameter flat-faced electrodes are used for this joint type. The second joint welded a set of wires placed parallel to one another. The electrodes were contoured to provide concentration of weld current and displacement needed for bonding.

The resistance mash welding process depends on developing enough heat in the base metal to be joined, preferably at the faying interface, to soften the metal. The timing of the weld schedule is set so that once the metal has softened, the weld force is rapidly increased to induce the required deformation. A conventional spot welding machine may have significant mass or friction in the guides that limit the dynamic response associated with rapid changes in weld force. To improve upon this inertial effect, the upper electrode of the welder was replaced with a fast follow-up head. A schematic of the head used is shown in Figure 5. The electrode is mounted on a low mass structure that is guided on a low friction support, the entire assembly is spring loaded with Bellville washers. The operation of the head is quite simple, as the welder pressure is applied to the head, the Bellville washers collapse and transfer the load to the copper wires. As the copper heats and softens, the washers allow the structure to expand and follow the collapse of the copper; the low mass of the structure insures that this response is immediate.[2,4-10] The initial weld trials for this project were done using and electric servo-driven resistance spot welding gun. This type of weld gun uses a lead screw and an electric motor to create the weld force. The initial results showed that the response time of this system was unstable. As a result, the remainder of the trials were done using a more conventional pneumatic spot welder with the fast follow-up head.

Procedure

Materials

The wires in this study were rectangular in cross section and measured 3.44 × 3.66 mm. Predominately, C101 copper wires were used, but some weld trials were also performed with C110 copper wires. Wires were welded with two geometries, referred to as crossed and parallel, as described below. All welds were performed on the 3.66-mm faces of C101 copper wire.

Equipment

Two welding machines were used in this study. The initial machine was a 60-kVA medium-frequency direct current (MFDC) servo-gun produced by ARO. As described above, the lack of follow-up capability and the inability to integrate a separate follow-up system within the servo-gun control scheme promoted the use of a more traditional pneumatic system.

The second welder, used for most of the study, was a 40-kVA MFDC system with a Miyachi ISA 500 AR controller integrated with a RWMA Size 2 pedestal-type frame. The pneumatic system provided weld and forge capability and was programmable to within ±2 ms by the controller. The weight of the ram was calculated to be 622 N (140 lb). Several adjustments were made to

the operation of the welder during the course of the investigation. These changes included loosening the slides on the ram to allow the head to fall more freely; adjustment of various throttling values to provide a soft touch at the initial electrode contact [~225-N (50-lb) force] followed by a build up to the electrode force; and reducing the air cylinder bore size to allow better control over the air pressures regulating the weld and forge forces.

Three styles of electrodes were used. The first was a 15.8-mm (⅝-in.)-diameter, male, flat-faced electrode (Type C)[11] , which was predominately used with the cross-wire geometry. The other two electrode designs were non-standard. These were produced from 19-mm (¾-in.)-diameter Type C electrodes machined to the dimensions shown in Figures 6 and 7. The 3-mm flat was designed to avoid substantial yielding the copper [80-MPa (11.5-ksi) nominal pressure] with 800-N (180-lb) weld force. The angles (30 and 45 degrees) were selected to provide current and forge force concentration within the 15.8- × 15.8-mm (⅝- × ⅝-in.) cross-sectional footprint. The electrode materials were all produced from RWMA Class 20 AL-60 material supplied by Luvata (formerly Nippert). This material was chosen for its anti-sticking properties and good electrical conductivity.

A single weld fixture design was used in this investigation to position the wires for welding; shown in Figure 8. The wires for the parallel-wire joint geometry were bent to a 112-degree angle using the fixture shown in Figure 9. The stripped end of the narrow width of the wire was inserted into the gap in the fixture and manually bent around the 5-mm (0.197-in.) radius machined into the fixture.

A fast follow-up head was required in this system due to the rapid softening and collapse of the copper wires during welding. Without the system, the large inertia of the weld machine ram resulted in a loss of weld force at the faying and electrode-wire interfaces, leading to overheating and massive expulsion of metal from these locations. The fast follow-up head design used in this study is shown in Figure 5. Belleville washers were used as springs. The geometry, number of washers, and the orientation of the washers define the spring constant and maximum displacement of the system. The springs were lubricated with molybdenum-bearing grease during assembly. A hardened shoulder bolt provided alignment of the washers.

The original design of the head incorporated a Teflon sleeve-bearing system; the head was upgraded during the program to use linear bearings to improve dynamic head motion. The tooling attached to the lower plate of the head was also modified to reduce weight and directly hold the electrodes described previously. The displacement motion within the fast follow-up head was monitored using a linear potentiometer described below.

Another improvement made to the head was incorporation of a force shunt, which engaged only during the forge portion of the weld schedule. Previously, forging of the wires could not initiate

until the Belleville washers were fully collapsed by the buildup of forge force. However, full collapse of the washers could lead to marring of the shoulder bolt surface, leading to a loss of repeatability and poor follow-up behavior. By inclusion of the force shunt, the forge initiation occurred earlier, before the washers had fully collapsed. The level of forge force buildup prior to engaging the force shunt was adjustable to within 0.076 mm (0.003 in.).

Data Acquisition, Monitoring, and Test Equipment

Both peak weld current and electrode force were recorded for all the weld trials. A calibrated Miyachi 326B weld current monitor was used to measure the peak current. Static force was measured using a hand held 45-kN (10,000-lb) strain gauge-based force gauge.

Dynamic weld current, voltage, and two displacement measurements were captured using a 16-bit Yokogawa DL750 ScopeCorder. The entire setup of the test system is shown in Figure 10. The data acquisition rate was 5 and 10 thousand samples/second (ksps). The current signal was acquired from the output of the Miyachi current meter and calibrated to the peak current measurements at several different weld current levels. Two displacement measurements of were made using linear potentiometer sensors. One measurement monitored the platen movement within the fast follow-up head. The second measurement monitored the displacement between the base of the fast follow-up head and the lower electrode position across the wires. The displacement sensors were calibrated over the ranges of interest by the static measurements of shims of known thicknesses. The displacement measurement made within the fast follow-up head was converted to weld force by empirically measuring the spring constant for the fast follow-up system.

The test used in this investigation to describe weld quality was load. A calibrated 20-kip Baldwin-Satec hydraulic tensile test unit with several load ranges was used in this investigation.

Experimental Approach

The weld schedule was based on a weld and forge methodology.[7] Previous experience in resistance welding copper at EWI has shown this to be the best approach for high-volume applications with minimal damage to the insulation.

The weld schedule was developed by evaluating the results from a series of iterative trials. Selection and scaling of the variables for each set of iterations was based on prior experience and knowledge of the process. The other variables were kept constant during a specific set of tests. These trials included iterations of such variables as:

- Weld force

- Forge force
- Timing between weld and forge initiation
- Weld current
- Weld time
- Pre-weld parameters
- Cool times
- The length of stripped wire (5 mm vs. other)
- Degree of insulation stripped from wire
- Placement location of wire relative to chisel tip location
- Method of wire surface preparation
- Equipment examinations, including fast follow-up head design

Both cross and parallel joint configurations were welded in the program using the same weld fixture, shown in Figure 8. The cross joints used flat faced electrodes while the parallel-wire geometry used the chisel faced electrodes (Figures 6 and 7). Nominally, 5 mm of the wire end was stripped of insulation using a fine cylindrical rasp actuated by a pneumatic drill. For the parallel-wire arrangement, each wire was bent to a 112-degree angle using the bend fixture (Figure 9). The wires were then placed in the weld fixture (Figure 8). The wires for the cross-wire geometry were extended approximately 10 mm beyond the cross location. The wires for the parallel-wire geometry were aligned such that the edges of the stripped ends of each wire were aligned and the straight ends of the wires were placed over top of one another. Then, each wire was tightened against the fixture using a nylon-tipped set screw. The assembled weld fixture was placed on the base attached to the lower electrode. The stripped edge of the wire was positioned at the operator side of the electrode face width. To accommodate the reduction in joint thickness during welding, a spacer wire was temporally placed under the weld fixture to elevate it during the squeeze portion of the weld schedule. The spacer wire was removed after the weld force built up, but before initiation of the weld. Finally, the electrodes were flood cooled during welding. This was necessary because the fast follow-up head did not incorporate water cooling capability.

Weld Quality Test Methods

Weld quality was characterized by the visual inspection, final weld thickness, tensile properties, metallographic examination, and weld repeatability.

The weld joint was visually inspected immediately after the weld process. Wire alignment, weld placement within the joint, bulging of the weld width, and other features of the weld were examined prior to destructive testing. This inspection included measurement of the final joint thickness using calibrated digital calipers at the center of the electrode impression on the wires.

Post-test inspection included assessment of straightening of the weld joint during tension, examination of the fracture surface, and other observations related to wire sliding, metal expulsion, etc.

Tensile tests were performed on the shop floor for most of the weld trials. The welded sample was prepared by gripping the wire away from the 112-degree bend with pliers and bending the adjacent sections of wire (away from the joint) perpendicular to the weld axis, as shown in Figure 11. The tensile test rate was 50 mm/min. During testing, the wire was free to twist the grips about the sample length axis. The peak tensile load was measured for each weld during procedure development. Generally, high peak loads were associated with extensive elongation of the test sample due to straightening of the 112-degree bends placed in the wires prior to welding. Welds of lesser peak tensile strength often failed while straightening the wires and rotating the tensile grips. Rotation of the wires in-plane with the flaying interface was also observed for some welds (mostly weak welds). Weld failure occurred either by twisting in the faying plane (shear) or button pull (separation of the ligament of wire thinned during welding from the adjacent welded region).[12] Tensile load built rapidly once the wires were straightened [generally over about 445 N (100 lb)].

Metallographic examinations were also used to characterize weld quality. Welds from selected trials were prepared and photographed using standard metallographic techniques. A Ferric Cloride and HCL etchant was used to examine the microstructure. Microhardness maps were developed using a Leco AMH-43 automatic hardness tester. The indents were made with a 0.25-mm spacing in both X and Y directions. Hardness evaluations were done with a 100-g load and a Vickers indenter with 10-s dwell time.

Achievement of an acceptable weld schedule was also defined by assessing the consistency of the weld strength and final thickness. Replicate welds were made for sets of welds with identical welding conditions and parameters. These were assessed using mean, range, and standard deviation statistics. A weld schedule that achieved high average peak strengths, a relatively small minimum to maximum range, and final wire thicknesses greater than 2 mm was considered acceptable.

Results

The results are reported by cross- and parallel-wire orientations, as well as by the welding unit used in the investigation in the subsequent sections below.

Cross-Wire Weld Trials

The weld schedule for the cross- and parallel-wire geometries were largely developed using a pneumatic welder, but the initial development work was performed on a servo-gun.

The parameters, weld thickness, and tensile results for the welds performed on the servo-gun are listed in Table 1. The table shows weld parameter iterations of weld time, weld current, weld force, forge force, pre-weld, and anneal (pulse welding) parameters (see Figure 2). The first 20 trials provided initial scaling of the weld variables. Additionally, the ability of a pre-weld to effectively remove any remaining insulation from the weld area was investigated over these first trials. These trials showed that a long duration/low current pulse could remove at least a minimal amount of insulation residual from the cleaning process.

Weld Trials 1 to 33 were performed on the cross-wire geometry. Trials 34 to 41 were performed on the parallel-wire arrangement. Relatively high electrode forces were used in these trials compared to trials performed on the pneumatic equipment. The anneal portion of the schedule served as the weld impulse in these trials. The best weld tensile strength was obtained on the cross-wire geometry using this equipment, with joint strengths up to 900 N (200 lb). Conversely, welds made in the parallel-wire geometry achieved less than 270-N (60-lb) tensile strength. All of these trials used flat-faced electrodes.

The follow-up capability of the servo-gun was found to be insufficient to keep from expelling metal from the joint interfaces. Additionally, the force feedback algorithm was not compatible with the inclusion of an external fast follow-up head. Consequently, work on this project migrated to the pneumatic weld unit.

The weld trials performed with the pneumatic weld unit are grouped into the following sequences:

(1) Weld schedule development on the cross-wire weld geometry
(2) Weld equipment modifications
(3) Weld schedule development on the parallel-wire geometry.

The weld data for these three sets of weld trials are given in Tables 2 to 4, respectively.

Table 2 lists the results of weld trials performed on the cross-wire joint geometry on the pneumatic weld unit with flat-faced electrodes. Similar to Table 1, the data in Table 2 includes iterative variations in the weld, forge, forge timing, and other weld schedule and wire parameters investigated, as well as final weld thickness and tensile strength results. Generally, the tensile strength of the welds increased as the values for weld time, weld force, and forge force all decreased and the weld current increased.

As illustrated in Weld 63, the best welding parameters for the cross-wire geometry was:

- Electrode Design: Flat-faced 15.8-mm (⅝-in.)-diameter electrodes
- Weld Force: 710 N (160 lb)
- Weld Time: 50 ms
- Weld Current: 31 kA
- Forge Delay Time: 40 ms
- Forge Force: 5.33 kN (1200 lb)

Welds with the cross-wire geometry using this schedule achieved tensile strength values between 1.44 to 1.60 kN (325 to 360 lb) with longer weld time; however, these welds were subject to wire-electrode sticking. Consequently, the weld time was reduced in an effort to reduce/eliminate the sticking tendency. By reducing weld time, electrode force, and forge force, welds of similar quality could be obtained by adjusting weld current without encountering the level of sticking that had been previously observed. Additional trials in Table 2 include data on copper alloys (C101 vs. C110), two-high cross tension weld joints, and use of TZM spacers between pairs of copper wires. Welds using the TZM spacers demonstrated that two pairs of wires could potentially be welded using the same welding parameters established for a single pair of wires. Weld trials involving both the C101 and C110 compositions showed that there is no apparent difference in welding requirements between these wire compositions.

Parallel-Wire Weld Trials

Table 2 also lists several results from the parallel-wire geometry. These are included in Trials 66 to 75. The variations in welding parameters for these trials largely followed the parameter ranges established on the cross-wire geometry. Similar to the trials performed on the servo-gun, the weld strengths in these trials were not as high as those produced on the cross-wire joints. The best welds in this part of the investigation were achieved by balancing the weld time and current to provide between 540- and 800-N (120- and 180-lb) tensile strength. This joint geometry was also subject to sticking at long weld times, but sticking was again reduced at the shorter times.

A new electrode design was developed specifically for welding the parallel-wire joint geometry (Figure 6). However, the new electrode design exposed operational issues with the fast follow-up head attributed to the asymmetric loading and excessive wear of the Teflon bearing sleeve. A symmetric electrode design was developed and is shown in Figure 7. This design resolved concern over asymmetric loading of the bearings in the fast follow-up head. Further welder issues were also encountered that interfered with development of the weld schedule for the parallel-wire joint. Table 3 nominally lists the welding trials that evolved during the discovery of equipment-related issues and their resolution. Issues with the operation of the fast follow-up

head and sticking of the ram (this issue was noted in later trials, shown in Table 4) are specifically discussed below. Initial weld repeatability issues were also investigated as part of this portion of the work.

Identification of Sources of Variability in Weld Tensile Strength

Trials 83 through 100 largely dealt with adjustments to the new electrode design and tooling. Trials 101 to 105 evaluated incremental changes in forge initiation time, weld current, weld time, and electrode force. Starting with Trial 108 a new fast follow-up head was implemented. This head included ball-bearing slides replacing the Teflon sleeves. The new unit was able to better handle both vertical and side loading which almost completely eliminated expulsion of metal and destruction of the electrode faces previously observed with the Teflon sleeve unit. After making adjustments to the welding parameters to further resolve electrode sticking (use of current pulsing) and improve weld strength (weld current and forge initiation time adjustments), weld tensile strengths in excess of 1,33 kN (300 lb) were obtained. Weld Trials 120 to 144 examined weld strength repeatability. While good weld strengths could be obtained [values greater than 1.11 kN (250 lb)], the variability in strength was significant.

Weld strength variability was, in part, due to the size of the air cylinder (101.6-mm (4-in.) bore diameter), which made it difficult to precisely control the applied force. This size of cylinder required only a 10-kPa (1½-psi) difference in air pressure between the upper and lower chambers to produce the weld and forge values desired. By switching to a much smaller cylinder [38.1-mm (1.5-in.) bore diameter] in Trial 154 (Table 4), the air pressure was scaled more appropriately [210 to 480 kPa (30 to 70-psi)] and resulted in much more repeatable force values. However, there was still significant variability in weld strength.

Another cause of variability was thought to be the delay in the onset of the full forging force due to the spring response of the Bellville washers. This was a potential issue in both the Teflon sleeve and linear bearing follow-up heads. In these systems, forging was not effective (actual deformation of the wires) until the Belleville washers had been completely flattened by the initial application of the forge force (which loaded the washers to their full capacity). In order to adjust the forge timing, an additional modification was made to the linear bearing fast follow-up head (starting with Trial 154 in Table 4). This was accomplished by shunting the forge force past the washers after a set level of washer displacement had been produced (user adjustable). In this way, the forging action was applied directly to the wires rather than mixed between wire deformation and washer collapse. This modification helped to preserve the integrity of the center post and allowed direct control over the timing of the forge while enabling the benefits of fast follow-up. However, the delay in the onset of the actual forging action was not found to be the major cause of variability in weld strength.

Significant variability in weld strength performance was found to be related to marring of the center post surface of the fast follow-up head. The center post keeps the Belleville washers aligned during use. Marring of the surface prevents the washers from moving freely. The Teflon sleeve bearing was sufficiently worn to cause the washers to rub along the scarred surface of the center post enough to prevent the passage of current and cause of metal expulsion at the wires and electrode surfaces. This is illustrated in Figure 12. After the center post was changed, the weld head motion was notably smoother and the welds were more repeatable.

Finally, repeatability was also harmed by sticktion (combination of sticking and friction) between the welder ram and the ram guides. This factor was not identified until relatively late in the weld schedule development on the parallel-wire geometry, as seen in Table 4. This issue was addressed after Trial 198. Plots of the fast follow-up head displacement versus applied force, both with and without sticktion, are shown in Figure 13. It is unknown when degradation of the ram (creating sticktion) became an issue, or the extent to which it influenced the results. However, similar to the marred center posts, this issue prevented repeatable applications of weld and forge forces, and appears to have been a significant contributor to weld strength variation.

Parallel-Wire Weld Schedule Development Trials

The majority of the parallel-wire joint geometry weld schedule development results are presented in Table 4. Table 4 also includes various adjustments made to the air throttle value (affecting the ram approach rate), corrections to the ram guide position, and installation of the forge force shunt modified fast follow-up head. The ability to adjust the timing of the forge force enabled a number of weld trials investigating the influence of actual forge initiation time on weld strength and consistency. The best setting for the forge force shunt position was 47.62 mm (1.875 in.) (relative, arbitrary measurement on the unit). This setting initiated forging of the wires shortly after the end of the weld time but well before complete collapse of the washers.

Generally, the data in Table 4 shows that higher strength welds were produced when the weld and forge forces decreased, the weld impulse times increased, and the inter-pulse cool times increased in these trials compared to the values listed in Table 3.

The best weld schedule for the parallel-wire joint (Trials 226 to 240) was:

- Electrode Design: 3-mm face width, 30-degree angle, 15.8-mm (⅝-in.) square electrodes
- Weld Force: 800 N (180 lb)
- 1st Weld Impulse: 24 ms

- 1st Impulse Current: 24.5 kA
- Cool Time: 8 ms
- 2nd Weld Impulse: 17 ms
- 3rd Impulse Current: 24.5 kA
- Cool Time: 8 ms
- 3rd Weld Impulse: 17 ms
- 3rd Impulse Current: 24.5 kA
- Forge Delay Time: 42 ms
- Forge Force: 2.14 kN (480 lb)
- Forge initiation time: within 10 ms of the cessation of current

This weld schedule produced weld tensile strengths between 780 N and 1.65 kN (175 and 370 lb) over 14 welds with an average strength of 1.10 kN (247 lb).

Figure 14 shows the dynamic voltage, dynamic current, displacement in the fast follow-up head, dynamic electrode force (measured from displacement values within the fast follow-up head) and dynamic resistance measured during Weld 226. The current signal shows the pulsed nature of the weld current. Pulsation is also observed in the voltage signal. In addition, the magnitude of the voltage decreases with each pulse. The displacement measurement shows the effects of thermal expansion followed by indentation of the electrode into the wires and lateral expansion of the copper within the joint. The electrode force measurement shows the effective force falling with each change in collapse of the wire consistent with the behavior of the fast follow-up head motion. At the cessation of current, the forge force initiates and builds force until the force shunt applies force directly to the joint, bypassing the fast follow-up head. Finally, the dynamic resistance primarily illustrates the changes in voltage across the weld. These changes are directly related to thermal expansion within each pulse, thinning of the wire, and increased bulk resistivity.

Table 4 also lists several sets of welds used to investigate consistency of weld strength for a fixed set of weld parameters. The sets of welds considered in this analysis were:

- Welds 129-139 (Table 3)
- Welds 192-197
- Welds 199-203
- Welds 215, 218-223
- Welds 226-239

Test procedures in Minitab 15™ were used to compare the means and variances for weld tensile strength and final weld thickness for the sets of parallel-wire joints above. The variability in these measures were investigated using one-way ANOVA techniques.

Tables 5 and 6 provide one-way ANOVA statistics comparing the means weld strength and final weld thickness. The data in these tables show that at least one mean is different from the others being compared. The text chart illustrating the confidence intervals for each set shows that final weld thickness for the Weld 226-239 dataset is about 2.5 mm with an average strength of about 250 lb. This dataset represents the best-practice weld schedule. The other datasets represent less effective weld schedules. These generally had wider 95% individual confidence intervals (an indicator of decreased precision).

Metallographic Data

Welds 63 and 240 were selected for detailed metallographic examination. Welds 63 and 240 represent the best weld schedules for the cross- and parallel-weld geometries, metallographic results for these welds are presented in Figures 15 and 16. Weld 63 was sectioned parallel to the face of the weld fixture and Weld 240 was sectioned transverse to the weld fixture. Micro-hardness maps of the cross sections of Welds 63 and 240 are presented in Figures 17 and 18.

The section of the cross-wire geometry (Figure 15) shows areas of grain refinement (previous forged structure) in a predominately equiaxed microstructure. The refined regions are nominally in areas adjacent to the electrodes. Additionally, Figure 17 shows that the hardness is fairly uniform through most of the cross section, except for a softened region along the bond line. In addition, there were harder regions adjacent to the welding electrodes. In these regions, it is believed that thermal constraints provided by the electrodes minimized recovery/recrystalization, leaving localized harder regions in the weld microstructure.

Figure 16 provides a similar cross section for the parallel-wire welding geometry. This micrograph shows a trend of grain coarsening both toward the left (free end) of the specimen, as well as toward the electrode faces themselves. Alternately, finer grain structures are evident both toward the bond line (between the electrodes) as well as into the wire bodies on the right side of the specimen. This change in grain structure is reflected in the hardness results. These results are presented in Figure 18. The hardness variations shown in Figure 18 essentially map out the grain size variations evident in Figure 16. It is of note that the maximum hardness for both Welds 63 and 240 is about 100 VHN. However, softening is more extensive in the parallel-weld (Weld 240). Minimum hardnesses in Welds 63 and 240 was 73 and 25 VHN, respectively.

Discussion

Weld and Forge Weld Schedule Approach

Pure copper is very difficult to resistance weld using the standard electrode force, current, and time recommended by the Resistance Welder Manufacturer Association (RWMA) and American Welding Society (AWS).[8,9,13] The inherently low bulk and surface resistances typical of high-conductivity copper promote the use of short time, very high current, and low electrode force weld procedures. However, these conditions cause electrode sticking, a factor limiting its weldability.[7-9,14-16] Despite these limitations, high conductivity copper products must still be joined together. Consequently, several welding techniques have been developed that compensate for these limitations, including:

- Resistance welding using refractory tipped electrodes (RWMA Class 10 to 14, composed of W, Mo, etc.)[6-9,14-16]
- Projection welding[5-8,12]
- Capacitive discharge welding[7,17]
- Resistance welding using a weld and forge approach.[7]

All of these methods have specific drawbacks. Welding with refractory-faced electrodes promotes electrode-sheet surface heating/melting and/or expulsion, deep indentation, and electrode deterioration.[6-9,14-16] Projection welding of pure copper requires additional maintenance of the projection geometry and control of electrode force.[5,7,10,12,18] Capacitive discharge welding of copper has been shown to be sensitive to weld time.[15] The weld and forge technique, common for welding aluminum, has been successfully used at EWI for welding pure copper; but, has little documentation in the literature.[7]

Although the refractory-faced electrode approach was briefly studied in the initial cross-wire welding trials of this investigation, the weld and forge technique was adopted for the following reasons:

- The refractory-faced electrodes produced expulsion from the electrode face-part surface interface.
- The refractory-faced electrodes appeared to increase electrode impression depth.
- The weld and forge technique appears to have a faster production cycle time.

In the present application, the cross-wire geometry is used as a type of projection weld since it concentrates both current and force using the part configuration. The parallel-wire geometry is a form of resistance welding since it uses the electrode face design to concentrate current and force. With both approaches, the low weld force levels in this study significantly increased the

heat generation at the faying surface without collapsing the joint.[7,15,16,18] After heating the weld zone to the forging temperature range using a specific current pulsation sequence, the application of forge force provides the deformation needed to strain the heated metal and produce a forge bond. Strains on the order of several hundred percent are required for bond formation.[3]

The weld current pulsing sequence allowed the heat generated at the faying interface to diffuse through the thickness of the joint and into the surrounding wire without overheating the faying interface. Relatively short heat times were used to limit the heat soak into the bulk wire and minimize damage to the insulation system. The weld times used are at least 25% shorter than those recommended for welding 0.9-mm sheet.[13] Based on average unit contact pressures, the weld force used in this study is approximately 20% less than that recommended for welding 0.9-mm sheet.

While the forge force produces a relatively high average unit contact pressure at the faying interface early in the forging operation for both the cross- and parallel-wire joint geometries, the average pressure continuously decreases as the contact area at the faying interface grows. The forging operation is slightly different for the cross- and parallel-wire joints in this study. The unit contact forge force exerted on the cross-wire joint during forging is largely controlled by the growth of rhombic-shaped interface between the wires. This surface area grows until the upper wire is fully collapsed into the lower wire. Forging is arrested due to the sudden increase in contact areas formed by doubling the wire surface area. This process produces significant strain at the joint interface. The parallel-wire surface area at the faying interface also grows with increased indentation of the electrode into the two wire thicknesses. Like the cross-wire joint, the collapse of the joint is arrested by the increased bearing surface area of the trapezoidal surfaces created by the electrode impressions and balanced against the hot compressive strength of the copper at the peak temperature within the joint.

Based on handbook values for hot tensile strength of C101 copper (assuming the compressive and tensile strengths are similar) and the calculated trapezoidal bearing surface areas of the electrode impressions as a function of indentation depth, the average temperature of the softest portion of the weld zone is approximately 450-500°C. This is based on a hot tensile strength of approximately 60.3 MPa (8750 psi) at 450-500°C.[19] This is consistent with the approximate forging temperature range of copper.[19] Additionally, the recrystalization temperature of C101 copper is approximately 300°C at 40% strain.[19] These temperature estimates are consistent with the areas of grain growth, grain refinement, forges structures, and hardnesses shown in Figures 15 to 18.

Given the correct combinations of weld force, weld time, forge force, and weld current for the parallel-wire geometry, a critical value of final joint thickness was observed in this study to

produce optimum weld tensile strength. A final joint thickness of 2.5 mm produces the highest weld strength as illustrated in Figure 19. This figure plots tensile strength as a function of final weld thickness for all of the tensile data obtained on the parallel-wire joint geometry in this study. The data for this plot comes from Tables 2 to 4 as noted in the plot legend. Two curves are drawn on the plot to help guide the eye. The curve on the right side of the distribution represents the upper bound indicative of the minimum forging strain required to produce welds of the indicated strength; i.e., without sufficient forging, the bond strength is reduced. The curve on the left side of the distribution represents the upper bound for strength lost due to excessive thinning of the wires by the electrode impression. These curves are upper bound values. The circled values at approximately 2.5-mm final joint thickness are replicate values from the best set of welding conditions (Trials 226 to 239).

Welding Requirements to Achieve Weld Strength Consistency

The weld and forge approach requires a repeatable, low electrode force and precise control of current to produce the heat required to forge the metal at the faying interface followed by a rapid application of forge force. Displacement of the weld head must respond equally rapidly to wire collapse during weld portion of the schedule to follow the dynamic changes in electrode height. The changes made to the fast follow-up system during these trials enabled the system to properly react to these changes. Without this capability, the weld produced expulsion, damage to the electrode face, and weld quality variability. Similarly, the ram must be capable of freely moving to produce the repeatable weld forces required. If the ram sticks, the force applied by the fast follow-up head will vary, again producing expulsion and damage to the electrode face.

Clearly, several factors (such as the ones list above) were shown to affect variability in the weld strength results. Corrections of these factors, in turn, resulted in improved repeatability. However, these results also suggest that heat sinking of the workpiece, associated positioning of the copper wires between the electrodes, also play a role. Figure 20 illustrates how variations in the extension of the free end of the wire past the electrode face affect the temperature within the joint prior to forging. If the extension of the free end of the wire is very short, heat from the weld flows into the wire and quickly heats this volume of metal. No additional heat will flow in that direction from the joint during welding, increasing the average temperature of the joint. Conversely, if extension of the end of the wire past the edge of the electrode is excessive, heat generated within the weld will flow into the wire end, decreasing the temperature of the weld zone. The amount of heat lost to the wire end will be proportional to the length of the wire extension. If the temperature of the weld zone drops sufficiently below the ideal forging temperature, the forge will become ineffective and result in a loss of joint strength. Variability in wire extension then is probably a major contributor to weld strength variability. Table 7 lists some of the weld trials examined to investigate the effects illustrated in Figure 20.

Recommended Weld Schedules

The recommended weld schedule for the cross-wire joint geometry is:

- Electrode Design: Flat-faced 15.8-mm (⅝-in.) diameter electrodes
- Weld Force: 710 N (160 lb)
- Weld Time: 50 ms
- Weld Current: 31 kA
- Forge Delay Time: 40 ms
- Forge Force: 5.34 kN (1200 lb)

The recommended weld schedule for the parallel-wire joint geometry is::

- Electrode Design: 3-mm face width, 30-degree angle, 15.8-mm (⅝-in.) square electrodes
- Weld Force: 800 N (180 lb)
- 1st Weld Impulse: 24 ms
- 1st Impulse Current: 24.5 kA
- Cool Time: 8 ms
- 2nd Weld Impulse: 17 ms
- 3rd Impulse Current: 24.5 kA
- Cool Time: 8 ms
- 3rd Weld Impulse: 17 ms
- 3rd Impulse Current: 24.5 kA
- Forge Delay Time: 42 ms
- Forge Force: 2.14 kN (480 lb)
- Forge initiation time: within 10 ms of the cessation of current

Conclusions

Weld schedules were developed for joining rectangular copper conductors in two relevant geometries, crossed and parallel. The process was capable of creating a reliable strong bond with no damage to the adjacent insulation. Specific findings are:

(1) Weld strengths using the recommended schedule for the cross-wire joint geometry were nominally greater than 1.56 kN (350 lb).

(2) Weld strengths using the recommended schedule for the parallel-wire joint geometry were nominally greater than 670 N (150 lb) and ranged between 750 N to 1.65 kN (170 and 370 lb).

(3) Bond line hardness using recommended weld schedules averaged approximately 73 to 78 VHN. This corresponds to an approximate weld temperature of 450-500^{o}C for the parallel-wire geometry based on typical hot tensile properties.

(4) Given the correct combinations of weld force, weld time, forge force, etc., the joint thickness was shown to be a critical variable for the parallel-wire geometry. The optimal final joint thickness was found to be 2.5 mm. The upper bounds for strength were related to critical forging strain and thinning of wire. Short weld times in this study produced inconsistent weld strength results, while longer weld times produced welds of acceptable strength and improved consistency.

(5) The welding equipment must be capable of providing smooth fast follow-up and weld force head motions. These are required due to the potential for rapid collapse of the wires during welding.

(6) Electrode sticking was minimized by the selection of the RWMA Class 20 electrode material, reduction in current, moderate weld times, and pulsation.

(7) The primary cause of weld variability in the tensile strength results appears to be variation in the length of the free end of the wire extending from the edge of the electrode. Excessive wire extension allows heat to flow from the joint, decreasing the average joint temperature and decreasing the efficacy of the forging operation. Conversely heat flow into a short wire extension saturates the volume of metal and increases the joint temperature prior to forging. Variations in wire extension were shown to have a dramatic effect on weld strength.

References

1. Agapiou, J.S., Perry, T.A. “Resistance mash Welding for Joining of Copper Conductors for Electric Motors,” *Journal of Manufacturing Processes*, Vol 15:549-557 (2013), Elsevier publishing
2. Hook, I. T., "The Welding of Copper and its Alloys," *Welding Research Supplement*, pp. 321-s-337-s (July 1955).
3. Gould, J. E., "Theoretical Analysis of Bonding Characteristics during Resistance Mash Seam Welding Sheet Steels," CRP Progress Report PR9807 (May 1998).

4. Gould, J. E., "Recent Advanced in Projection Welding," *EWI Insights*, Vol. 18.2.1 (Summer 2005).
5. Gould, J. E., "Projection Welding," *ASM Handbook*, Vol. 6 - Welding, pp. 230-237.
6. Fursov, V. A., "Improved Resistance Welding Technique for Electrical Leads," *Svar. Proiz.*, No. 3, pp. 36-38 (1966).
7. ASM Committee on Welding and Brazing of copper and Copper Alloys, "Resistance Welding of Copper and Copper Alloys," *Metals Handbook*, 8th Edition, Vol. 6 - Welding and Brazing, pp. 337-429 (1971).
8. "Procedure Development and Process Considerations for Resistance Welding," *ASM Handbook*, Vol. 6 - Welding, Brazing, and Soldering, pp. 849-850 (1993).
9. "Copper and Copper Base Alloys," Chapter 13, *Resistance Welding Manual*, 4th Edition, RWMA (1989).
10. Goodman, I. S., "Variables in Cross-Wire Welding of Dissimilar Metals," *Welding Journal*, pp. 863-875 (Oct. 1950).
11. "Specification for Automotive Resistance Spot Welding Electrodes" AWS D8.6:2005, American Welding Society (2005).
12. Dorn, L. and Stöber, E., "Microresistance Welding of wire Joints made from Different Metals," *Welding and Cutting*, No. 1, (1984).
13. "Elevated-Temperature Tensile Properties of C10100 or C10200 Rod, 1180 Temper, *Metals Handboo*k, Vol. 2, 10th Edition, Figure 1, p. 266 (1990).
14. Zhou, Y., Gorman, P., Tan, W., and Ely, K. J., "Weldability of Thin Sheet Metals during Small-Scale Resistance Spot Welding using an Alternating-Current Power Supply," *Journal of Electronic Materials*, Vol. 29, No. 9, pp. 1090-1099 (2000).
15. Tušek, J., Tuma, J. V., Jenko, M., and Pograjc, M., "Direct Resistance Projection Welding of Copper and Brass," *Science and Technology of Welding and Joining*, Vol. 10, No. 1 (2005).
16. Hollar, D. L., Jr., "Resistance Seam Welding of Thin Copper Foils," *Welding Journal*, pp. 37-44 (June 1993).
17. Paul, B. K., Wilson, D., McDowell, E., and Benjarattananon, J., "Study of Weld Strength Variability for Capacitor discharge Welding Process Automation," *Science and Technology of Welding and Joining*, Vol. 6, No. 2, pp. 109-115 (2001).
18. Jones, R. C., "Resistance Welding Crossed Wires," *Welding Journal*, 27 (12): 703-714 (1948).
19. "Spot Welding Parameters for Various Copper Alloys," *Recommended Practices for Resistance Welding*, AWS C1.1M/C1.1:200, Table 38, p. 40 (Jan. 31, 2000).

Table 1. Weld Trials Performed on the ARO Servogun

Weld ID	Weld Force (lbs)	Forge Force (lbs)	Weld Time (ms)	Weld Current (KA)	Weld Delay (ms, relative to start)	Pre-Weld Time (ms)	Pre-Weld Current (KA)	2nd Weld Time (ms)	2nd Weld Current (KA)	Thickness At Weld (mm)	Tensile Strength (lbs)	Comments
1	450	1349	80	20	490	0	0	0	0			
2	450	1124	80	25	490	0	0	0	0			expelled metal
3	674	1124	80	20	490	50	10	0	0			
4	674	899	0	0	490	50	10	0	0			
5	674	899	0	0	490	150	10	0	0			
6	674	899	0	0	490	200	10	0	0			
7	674	899	0	0	490	250	10	0	0			
8	674	899	0	0	490	175	10	0	0			
9	674	899	0	0	490	150	10	0	0			
10	674	674	80	25	490	150	10	0	0			
11	674	674	20	35	515	150	10	0	0			
12	674	899	10	40	520	150	10	0	0			
13	562	899	25	40	515	150	10	0	0			
14	450	674	30	30	520	150	10	0	0			
15	450	562	30	30	520	150	10	0	0			
16	551	1124	180	7	590	0	0	0	0			
17	551	1124	60	30	520	0	0	0	0			
18	551	1124	120	20	490	150	10	0	0			
19	551	1124	150	22	450	150	10	0	0			
20	551	573	100	22	450	150	10	0	0			Partial button
21	450	495	90	17	450	150	7	70	12	3.65	150	Shear
22	450	495	50	21	490	150	7	70	12	3.79	215	Shear
23	450	495	30	25	510	150	7	50	17	3.91	170	Shear
24	528	540	30	28	510	150	7	50	17	3.59	185	Shear
25	528	540	50	19	490	150	7	50	12			
26	382	393	50	20	490	150	7	50	12			Arcing - Destroy
27	382	540	65	19	520	0	0	40	24		105	Pulled button - E
28	382	540	65	19	570	0	0	40	24		180	Exp, complete s
29	382	540	65	17	570	0	0	40	23	4.15	155	Shear, Electrode
30	416	540	65	17	570	0	0	40	22	4.64	155	Shear, No Exp
31	405	540	65	18	570	0	0	40	22	3.79	170	Shear, Some Ex
32	416	584	65	17.5	570	0	0	40	25	3.61	180	Shear, No Exp
33	416	719	65	17.5	570	0	0	40	28	3.4	160	Shear, exp; Stra
34	472	719	65	15	570	0	0	40	20	3.52	45	Shear; Change t
35	450	719	65	17	570	0	0	40	20	3.8	55	Shear
36	427	719	65	18	570	0	0	40	21	2.92	50	Glow and Exp
37	416	629	65	17.5	570	0	0	40	22	4.05		Little Exp
38	450	562	65	19	570	0	0	40	25	4.66	30	Exp, complete s
39	540	629	65	19	570	0	0	40	25	5.61	30	
40	540	674	65	21	570	0	0	40	27			Exp, destroyed e
41	225	1349	80	9	570	0	0	60	40			Exp, destroyed e

Table 2. Weld Trials Performed on Pneumatic Welder while Developing the Cross-Wire Joint Welding Parameters

Weld ID	Weld Time (ms)	Weld Current (KA)	Force Weld (lbs)	Force Forge (lbs)	Exterior Water Cooling	Forge Current on Time (ms)	Measured Current (KA)	Final Thickness (mm)	Tensile Strength (lbs)	Comments
42	300	13	200	1620	No	70	14.45	3.88	0	Cross wire
43	300	17	200	1620	No	70	17.72	3.45	145	
44	350	17	200	1620	No	70	18.23	3.42	125	
45	200	21	200	1620	No	50		3.17	255	
46	200	22.5	200	1620	No	50	22.9	3.02	285	
47	200	24	200	1620	No	50	24.1	2.92	360	Electrode Sticking
48	200	26	200	1620	Yes	50		2.85	325	
49	200	29	200	1620	Yes	50	29.5	2.95	395	Pulled Button, Saw Glow
50	100	29	200	1620	Yes	-50		3.70	330	Saw Glow
51	100	29	200	1620	Yes	50	29.2	3.08	335	
52	70	31	200	1620	Yes	40	30.9	3.09	340	maximum Current Limit on Machine
53	70	30	200	1620	Yes	10	30	3.41	345	Saw Glow
54	140	30	200	1620	Yes	10	29.9	3.07	360	Saw Glow
55	50	20	175	1205	Yes	10	20.6	5.08	0	
56	50	25	175	1205	Yes	10	25.2	4.55	115	
57	50	27.5	175	1205	Yes	10	27.5	3.78	240	
58	50	29	175	1205	Yes	10	29.7	3.53	475	Pulled Button, Saw Glow - did not rotate until > 300lb
59	50	25	160	1205	Yes	10	23.4	4.62	135	
60	50	27.5	160	1205	Yes	10	27.7	4.30	165	
61	50	28.5	160	1205	Yes	10	28.5	3.72	335	
62	50	29.2	160	1205	Yes	10	31.3	3.84	470	
63	50	29.2	160	1205	Yes	10	31	3.63		Micro
64	50	20	175	1205	Yes	10		4.78	25	two sets of wires + TZM spacer
65	50	26	175	1205	Yes	10	27.1	3.82	225	Expulsion (TZM side) two sets of wires + TZM spacer
66	50	25	200	1620	Yes	10	26.9	3.99	10	Parallel Wire
67	50	30	200	1620	Yes	10	31.3	3.04	85	Parallel Wire
68	150	28	200	1620	Yes	110	29.5	1.34	65	Parallel Wire Exp, Sticking
69	100	28	200	1620	Yes	60		1.48	115	Parallel Wire Exp, Sticking
70	75	28	200	1620	Yes	10	29.9	2.65	175	Parallel Wire exp, Sticking, sliding of wires, Part
71	62	28	200	1620	Yes	10	30	4.39	50	Parallel Wire Minor sticking, wires sliding
72	100	24	200	1620	Yes	10	26.1	1.87	125	Parallel Wire Exp, Minor Sticking
73	100	20	200	1620	Yes	10	22.1	4.66	30	Parallel Wire
74	100	22	200	1620	Yes	10	24.2	2.94	70	Parallel Wire
75	60	30	200	1620	Yes	10	31.3	2.94	185	Parallel Wire Button, Possible exp
76	50	27.5	175	1205	Yes	10		4.22	340	C101 Copper Cross wire geometry
77	50	29	175	1205	Yes	10	30.6	3.97	460	C101 Copper
78	50	30.5	175	1205	Yes	10	32.1	3.78	495	C101 Copper
79	50	27.5	175	1205	Yes	10	29.3	4.38	335	C110 Copper
80	50	29	175	1205	Yes	10	30.7	4.15	380	C110 Copper
81	50	30.5	175	1205	Yes	10	32.2	3.90	400	C110 Copper

Table 3. Weld Trials Evaluating Weld Issues on the Pneumatic Welder on Both the Cross- and Parallel-Wire Joints

Weld ID	Weld Force (lbs)	Forge Force (lbs)	1st Pulse Weld Time (ms)	Cool Time (ms)	2nd Pulse Weld Time (ms)	Cool Time (ms)	3rd Pulse Weld Time (ms)	Forge Delay bigger is earlier (ms)	1st Pulse Current (KA)	2nd/3rd Pulse Current (KA)	Final Thickness (mm)	Tensile Strength (lbs)	Comment	
83	200	1620	50					10	29		4.38	60	Flat electrode design, Gain 4	Parallel wire geometry
84	200	1620	50					10	22.5			65	Manually ground chisel face and receiver electrode	
85	200	1620	50					10	26				Joint Slipped	
86	200	1620	50					10	26				Joint Slipped	
87	200	1620	50					10	26				Joint Slipped	Aligned Electrode Holders
88	200	1620	50					10	20			55	Flat and Chisel (Top) Electrodes	
89	200	1620	50					10	24			345	Miyachi Gain setting 8, Btn	May have exp
90	200	1620	40					10	22			245	Moved shelf down, BTN	Gain 9
91	200	1620	30					10	24			165	Blew up electrodes. Followup system problem	
92	210	1160	30					10	22				Blew up wires.	Adjusted flow valves
93	210	1160	50					10	22				Something wrong	
94	350	1160	50					10	22			65	Adjusted flow valves	
95	300	1160	50					10	26			65	Adjusted flow valves	
96	280	930	50					10	23			175	Adjusted flow valves	
97	280	930	75					35	17.5			55		
98	310	920	50					10	17		3.47		Sticking	
99	310	920	50					10	22.5		3.15	65		Gain 4
100	310	920	50					10	22.5		2.4	155	Minor Exp, Gain 8	Trialed various changes in springs and forces
101-1	310	640	50					50	22		3.14	110	Gain 8	
101-2	310	640	50					10	22		3.69	50	Gain 8	
101-3	310	640	50					70	22			0	Gain 8	
101-4	310	640	70					90	22			0	Gain 8	
101-5	310	640	70					70	22		3.11	90	Gain 8	
101-6	310	640	70					50	22		2.43	140	Gain 8	
101-7	310	640	70					30	22		2.48	75	Gain 8	
102-1	310	640	50					50	23		2.61	90	Gain 8	
102-2	310	640	70					50	23		1.25	160	Gain 8	
102-3	310	640	30					50	24		1.58	45	Gain 8	
102-4	310	640	50					50	23				Gain 8, Blew up electrodes	
103-1	310	640	50					30	18		1.53	40	Gain 8	Double Chisel Faced Electrodes
103-2	310	640	25					30	20		5.39	0	Gain 8	
103-3	310	640	25					30	22		5.3	0	Gain 9	
103-4	310	640	35					30	23		4.86	0	Gain 9	
103-5	310	640	35					30	23			0	Gain 9	390 flat load springs
104-1	240	530	50					30	14		0.99	100	Change Springs to 1200 lb flat load	
104-2	240	530	50					30	11		4.45	5		
104-3	240	530	50					30	12		4.2	30		
104-4	240	530	50					30	13		1.85	115		
104-5	240	530	50					30	12.5		1.67	135		
104-6	240	530	50					30	12		2.82	70		
105-1	220	430	25					30	15		4.95	105	Gain 4	Aligned tips, changed table height
105-2	220	430	25					30	16		6.15			
105-3	220	430	25					30	16		3.84	30		
105-4	220	430	25					30	17		4.22	20		
105-5	220	430	25					30	18		1.42	110	Extended sample, BTN	
105-6	220	430	25					30	17.5		3.92	60		
105-7	220	430	25					30	18.5				Blew up weld	
106	180	550	25					30	14		5.22	0		
107	180	550	25					30	16		5.15	200	Expulsion	
108	180	750	25					5	18			0	NEW FAST FOLLOW UP HEAD. New Pnumatic plumbing	
109	180	750	25					5	21			0	narrowed face width	
110	180	750	25					5	22		3.6	0		
111	180	750	40					20	22		1.74	65		
112	180	530	44					20	22		2.77	45	Changed Flow valve settings. Gain 7	
113	180	530	22	4	22			24	23		1.25	110	Gain 8, Btn	
114	170	440	11	4	11	4	11	32	23.2	22.5	3.2	60	4 pulses 11 on 4 off	
115	170	440	11	4	11	4	11	32	23.5	24	3.04	55	4 pulses 11 on 4 off	
116	170	440	22	3	14	3	14	32	23.5	24	3.05	70		
117	170	440	22	3	14	3	14	32	23.5	24	5.37	85	Turned off forge	
118	170	440	22	5	14	5	14	24	23.5	24	2.44	370	Forge on. Sticking, Btn	
119	170	440	20	5	13	5	13	20	23.5	24	3.09	325	Sticking, Btn	
120	200	450	20	5	13	5	13	14	23.5	24	3.86	60		
121	200	450	20	5	13	5	13	26	23.5	24	3.34	90	less Sticking	
122	200	450	20	5	13	5	13	20	23.5	24	3.71	40	much less sticking	
123	200	450	22	5	14	5	14	20	23.5	24	4.36	40	Blew up wires??	
124	200	450	22	5	14	5	14	20	21.5	21	4.28		Replaced electrodes. 3mm face	
125	200	450	22	5	14	5	14	20	23.5	23	3.65	55		
126	200	450	22	5	14	5	14	16	23.5	24	3.18	80	More glow	
127	200	450	22	5	18	5	18	20	23.5	24	3.45	145		
128	200	450	22	5	19	5	19	24	23.5	24	2.36	225	minor sticking	
129	200	450	22	5	19	5	19	24	23.5	23	3.25	110	minor sticking	replicate data
130	200	450	22	5	19	5	19	24	23.5	23	2.65	190		replicate data
131	200	450	22	5	19	5	19	24	23.5	23	2.35	270		replicate data
132	200	450	22	5	19	5	19	24	23.5	23	2.85	185		replicate data
133	200	450	22	5	19	5	19	24	23.5	23	2.7	170		replicate data
134	200	450	22	5	19	5	19	24	23.5	24	2.72	260		replicate data
135	200	450	22	5	19	5	19	24	23.5	24	2.75	205		replicate data
136	200	450	22	5	19	5	19	24	23.5	24	2.69	240		replicate data
137	200	450	22	5	19	5	19	24	23.5	24	2.92	140		replicate data
138	200	450	22	5	19	5	19	24	23.5	24	2.46	260		replicate data
139	200	450	22	5	19	5	19	24	23.5	24	2.69	175		replicate data
140	200	450	22	5	19	5	19	24	23.5	24	3.05	225	Changed centerpost. Adjusted flow vales for better "soft land". Still Gain 8	
141	200	450	22	5	19	5	19	24	23.5	24	2.63	285		replicate data
142	200	450	22	5	19	5	19	24	23.5	24	3.09	225		replicate data
143	200	450	22	5	19	5	19	30	23.5	24	2.65	295	Btn	replicate data
144	200	450	22	5	19	5	19	36	23.5	24	2.48	275	Btn	replicate data
145	200	450	22	5	19	5	19	34	23.5	24	3.63	90		
146	200	450	22	5	19	5	19	34	23.5	23.5	3.32	100		
147	200	450	22	5	19	5	19	34	23.5	24.5	3.27	100		
148	200	450	22	5	19	5	19	34	23.5	24	2.52	285	Btn	
149	200	450	22	5	19	5	19	34	23.5	24	2.71	465	Chisel faced electrdes, Btn	Cross Wire
150	200	450	22	5	19	5	19	34	23.5	24	2.44	340	Btn	Cross Wire
151	200	450	22	5	19	5	19	34	23.5	24	2.64	345	Btn	Cross Wire
152	200	450	22	5	19	5	19	34	23.5	24	2.9		Sample	Parallel
153	200	450	22	5	19	5	19	34	23.5	24	2.75		Sample	Cross Wire

Table 4. Weld Trials Performed on Pneumatic Welder while Developing the Parallel-Wire Joint Welding Parameters

Weld ID	Weld Force (lbs)	Forge Force (lbs)	Stop Set (in)	1st Pulse Weld Time (ms)	Cool Time (ms)	2nd Pulse Weld Time (ms)	Cool Time (ms)	3rd Pulse Weld Time (ms)	Forge Delay bigger is earlier (ms)	1st Pulse Current (KA)	2nd/3rd Pulse Current (KA)	Final Thickness (mm)	Tensile Strength (lbs)	Comment
154	190	500	2.026	22	5	19	5	19	34	22.5	22.5	0.71		
155	190	500	1.976	22	5	19	5	19	34	21.5	21.5	0.83	45	Btn
156	190	500	1.970	22	5	19	5	19	34	19.5	19.5	1.78	210	Btn
157	190	500	1.923	22	5	19	5	19	34	18	18	1.54	160	Btn
158	190	500	1.903	22	5	19	5	19	34	17	17	2.82	100	Shear
159	190	500	1.903	18	5	18	5	18	34	18	18	3.61	70	Shear
160	190	500	1.875	17	5	17	5	17	34	20	20	5.61	0	INSULATION in joint
161	190	500	1.875	16	4	16	4	16	34	21	21	1.51	230	Btn
162	190	500	1.875	12	3	12	3	12	34	22	22	2.55	125	Shear
163	190	500	1.875	8	2	8	2	8	34	24.5	24.5	2.55	340	Btn
164	190	500	1.875	12	3	12	0	0	33	24.5	24.5	2.44	315	Shear
165	190	500	1.875	20	0	0	0	0	26	24.5		3.63	110	Low voltage, Sticking
166	190	500	1.875	20	0	0	0	0	26	24.5		4.26	60	Shear
167	190	500	1.850	10	2	8	2	8	30	24.5	24	3.53	80	Shear
168	190	500	1.850	10	2	8	2	8	15	24	24.5	3.61	125	Shear
169	190	500	1.850	10	2	8	2	8	45	24	24.5	3.02	125	Shear
170	190	500	1.850	10	2	8	2	8	36	24	24.5	3.28	75	Shear
171	190	500	1.875	10	2	8	2	8	34	24	24.5	3.52	80	Shear
172	190	580	1.875	12	3	12	3	12	36	24	24.5	0.98		
173	190	580	1.875	10	2	8	2	8	34	21.5	21.5	3.1	140	Shear
174	190	580	1.875	10	2	8	2	8	30	22.5	22.5	3.6	75	Shear
175	190	580	1.875	10	2	8	2	8	38	22.5	22.5	3.55	60	Shear
176	190	580	1.875	10	2	8	2	8	34	23	24.5	2.19	140	Shear
177	190	580	1.875	10	2	8	2	8	34	23.5	24	2.01	140	Shear
178	190	580	1.875	10	2	8	2	8	30	23.5	23.5	2.23	270	Btn
179	190	580	1.875	10	2	8	2	8	30	23	23.5	2.82	60	???
180	190	580	1.875	10	2	8	2	8	30	23	23.5	2.85	165	Shear
181	190	580	1.875	12	2	8	2	8	32	23.5	23.5	2.73	85	Shear
182	190	580	1.875	14	2	10	2	10	38	23.5	23.5	1.66	210	Btn
183	190	580	1.875	8	2	8	2	8	33	24	24	2.1	260	Btn
184	190	550	1.875	8	2	8	2	8	33	24	24	4.06	75	throtle valve change
185	190	550	1.875	8	2	8	2	8	33	24	24	3.76	95	throtle valve change
186	190	570	1.875	8	2	8	2	8	33	24	24	4.6		throtle valve change
187	190	570	1.875	8	2	8	2	8	33	24	24	3.16	50	throtle valve change
188	190	580	1.875	12	2	8	2	8	33	24	24	1.03		throtle valve change
189	190	580	1.875	10	2	8	2	8	33	24	24	3.37	70	throtle valve change
190	190	580	1.875	10	2	8	2	8	27	24	24	3.28	70	
191	190	580	1.875	14	2	9	2	9	23	24	24	3.7	90	
192	190	580	1.875	14	2	12	2	12	22	24	24	2.26	275	
193	190	580	1.875	14	2	12	2	12	22	24	24	2.25	235	
194	190	580	1.875	14	2	12	2	12	22	24	24	1.36	75	
195	190	580	1.875	14	2	12	2	12	22	24	24	2.73	90	
196	190	580	1.875	14	2	12	2	12	22	24	24	2.31	175	
197	190	580	1.875	14	2	12	2	12	22	24	24	2.96	130	
198	190	580	1.875	10	2	8	2	8	25	24	24	4.65	40	Changed Right Side Guide of Ram
199	190	580	1.875	14	2	12	2	12	22	24	24	2.49	165	
200	190	580	1.875	14	2	12	2	12	22	24	24	2.89	60	
201	190	580	1.875	14	2	12	2	12	22	24	24	2.11	270	
202	190	580	1.875	14	2	12	2	12	22	24	24	2.54	240	
203	190	580	1.875	14	2	12	2	12	22	24	24	3.6	60	
204	190	580	1.875	20	2	8	2	8	22	23.5	24	3.4	55	
205	190	580	1.875	24	2	12	2	12	22	23.5	24	1.11	60	Btn
206	190	490	1.875	24	2	12	2	12	22	23.5	24	2.15	145	
207	180	480	1.875	24	2	12	2	12	22	24	24	0.4		
208	180	480	1.875	24	2	12	2	12	22	21	21	3.27	45	
209	180	480	1.875	24	2	12	2	12	22	23	23	1.7		
210	180	480	1.875	24	2	12	2	12	22	22	22	2.67	70	
211	180	480	1.875	15	2	15	2	15	22	23	23	2.27	50	
212	180	480	1.875	15	4	15	4	15	23	23.5	23.5	2.51	105	
213	180	480	1.875	15	5	15	5	15	23	24	24	2.85	115	
214	180	480	1.875	16	5	16	5	16	20	24.5	24.5	1.75		
215	180	480	1.875	16	8	16	8	16	22	24.5	24.5	2.66	160	
216	180	480	1.875	15	5	15	5	15	25	24.5	24.5	2.11	55	
217	180	480	1.875	15	5	15	5	15	25	24.5	24.5	2.64	145	
218	180	480	1.875	16	8	16	8	16	22	24.5	24.5	2.35	235	
219	180	480	1.875	16	8	16	8	16	22	24.5	24.5	2.85	60	
220	180	480	1.875	16	8	16	8	16	22	24.5	24.5	3.13	60	
221	180	480	1.875	16	8	16	8	16	22	24.5	24.5	2.3	225	
222	180	480	1.875	16	8	16	8	16	22	24.5	24.5	3.16	50	
223	180	480	1.875	16	8	16	8	16	22	24.5	24.5	3.15	45	
224	180	480	1.875	20	8	16	8	16	22	24.5	24.5	2.39	310	
225	180	480	1.875	22	8	16	8	16	22	24.5	24.5	2.63	180	
226	180	480	1.875	24	8	17	8	17	20	24.5	24.5	2.26	195	
227	180	480	1.875	24	8	17	8	17	32	24.5	24.5	2.74	290	
228	180	480	1.875	24	8	17	8	17	32	24.5	24.5	2.54	370	
229	180	480	1.875	24	8	17	8	17	32	24.5	24.5	2.22	310	
230	180	480	1.875	24	8	17	8	17	32	24.5	24.5	2.67	205	
231	180	480	1.875	24	8	17	8	17	32	24.5	24.5	2.14	280	
232	180	480	1.875	24	8	17	8	17	32	24.5	24.5	2.66	325	
233	180	480	1.875	24	8	17	8	17	32	24.5	24.5	2.41	305	
234	180	480	1.875	24	8	17	8	17	32	24.5	24.5	2.31	220	
235	180	480	1.875	24	8	17	8	17	32	24.5	24.5	2.69	205	
236	180	480	1.875	24	8	17	8	17	32	24.5	24.5	2.77	175	
237	180	480	1.875	24	8	17	8	17	32	24.5	24.5	2.92	195	
238	180	480	1.875	24	8	17	8	17	32	24.5	24.5	2.51	190	
239	180	480	1.875	24	8	17	8	17	32	24.5	24.5	2.39	205	
240	180	480	1.875	24	8	17	8	17	32	24.5	24.5	2.71		Micro

Table 5. ANOVA and Confidence Interval Statistics for Weld Strength from Replicate Parallel-Wire Joint Data in Tables 2 to 4

One-Way ANOVA for Strength Means

One-way ANOVA: Tensile Strength versus Weld Group

Source	DF	SS	MS	F	P
Weld Group	4	87714	21929	3.92	0.009
Error	38	212383	5589		
Total	42	300098			

S = 74.76 R-Sq = 29.23% R-Sq(adj) = 21.78%

Individual 95% CIs For Mean Based on Pooled StDev

Level	N	Mean	StDev	+---------+---------+---------+---------
129-139	11	200.45	52.22	(------*-------)
192-197	6	178.33	101.67	(----------*---------)
199-203	5	159.00	98.13	(-----------*----------)
215 218-223	7	119.29	85.22	(---------*--------)
226-239	14	247.86	62.84	(-----*------)
				+---------+---------+---------+---------
				60 120 180 240

Pooled StDev = 74.76

Table 6. ANOVA and Confidence Interval Statistics for Final Weld Thickness from Replicate Parallel-Wire Joint Data in Tables 2 to 4

One-Way ANOVA for Thickness Means

One-way ANOVA: Weld Thickness versus Weld Group

Source	DF	SS	MS	F	P
Weld Group	4	1.127	0.282	2.20	0.087
Error	38	4.868	0.128		
Total	42	5.996			

S = 0.3579 R-Sq = 18.80% R-Sq(adj) = 10.25%

Individual 95% CIs For Mean Based on Pooled StDev

Level	N	Mean	StDev	---+---------+---------+---------+------
129-139	11	2.7300	0.2344	(------*------)
192-197	6	2.3117	0.5491	(---------*---------)
199-203	5	2.7260	0.5614	(----------*----------)
215 218-223	7	2.7971	0.3728	(--------*--------)
226-239	14	2.5164	0.2349	(------*-----)
				---+---------+---------+---------+------
				2.10 2.40 2.70 3.00

Pooled StDev = 0.3579

Table 7. Additional Weld trials used to Investigate Effect of Excessive Wire Extension on Weld Strength

Weld ID	Wire Position	Final Weld Thickness (mm)	Tensile Strength (lb)
241-244	Unknown	1.91-2.38	200-250
245	Unknown	2.56	80
246	Very Long Extension: 6 mm	2.80	130
247	No Extension: 0mm	1.60	275
248	Standard Position: 1-mm Extension	2.08	310
249	Long Extension: 2- to 3-mm Extension	3.08	90

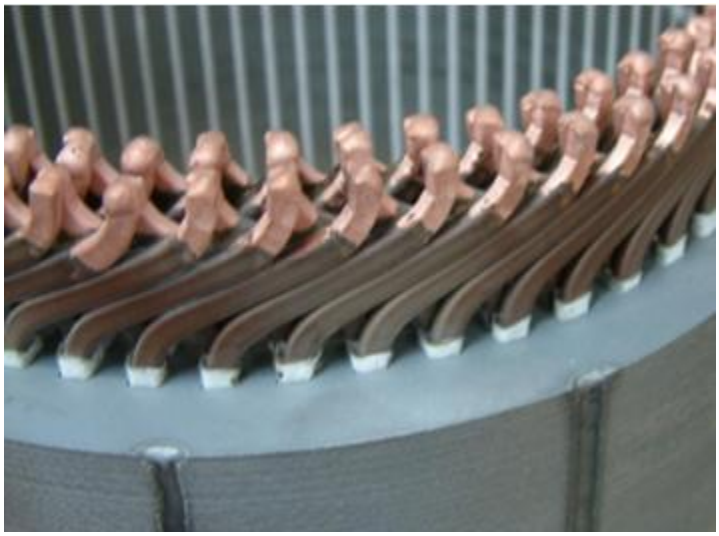

Figure 1. **Gas Tungsten Arc Welded (GTAW) Joints in Stator Assembly** [1]

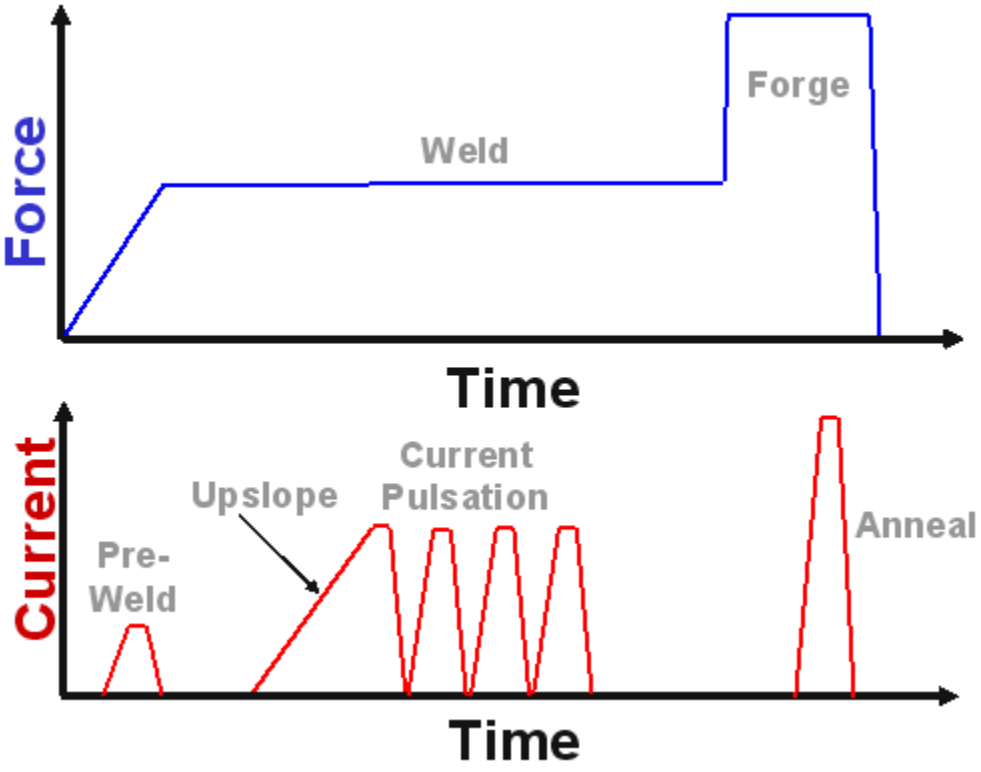

Figure 2. **Schematic Illustration of Typical Force and Current Variations for Resistance Welding Applications** (Example shows pre-weld, upslope, weld current pulsation, anneal current, weld force, and forge force.)

Figure 3. As-Welded Cross-Wire Joint Geometry

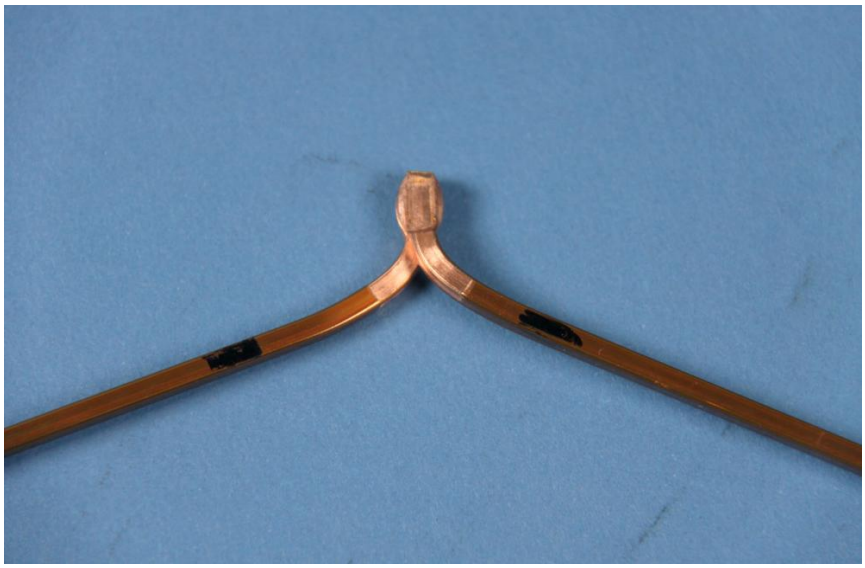

Figure 4. As-Welded Parallel-Wire Joint Geometry

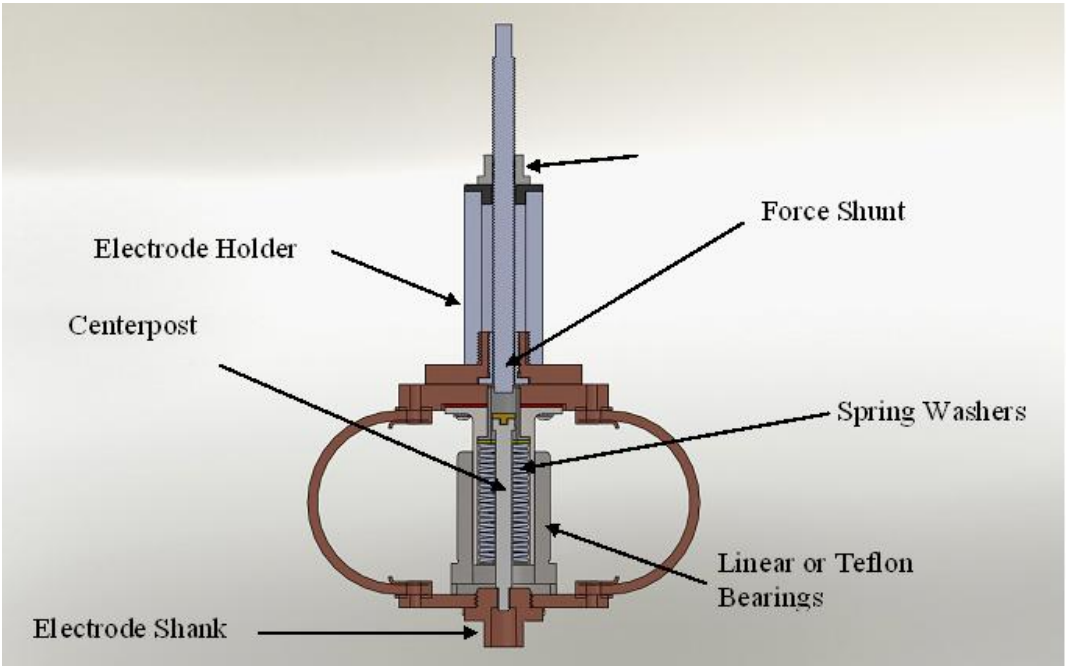

Figure 5. **Fast Follow-Up Head used in this Program** [Initial configuration used Teflon bearings, later replaced by linear bearings. Finally, a force shunt (center rod) was installed to set the level of effective forge force during welding.]

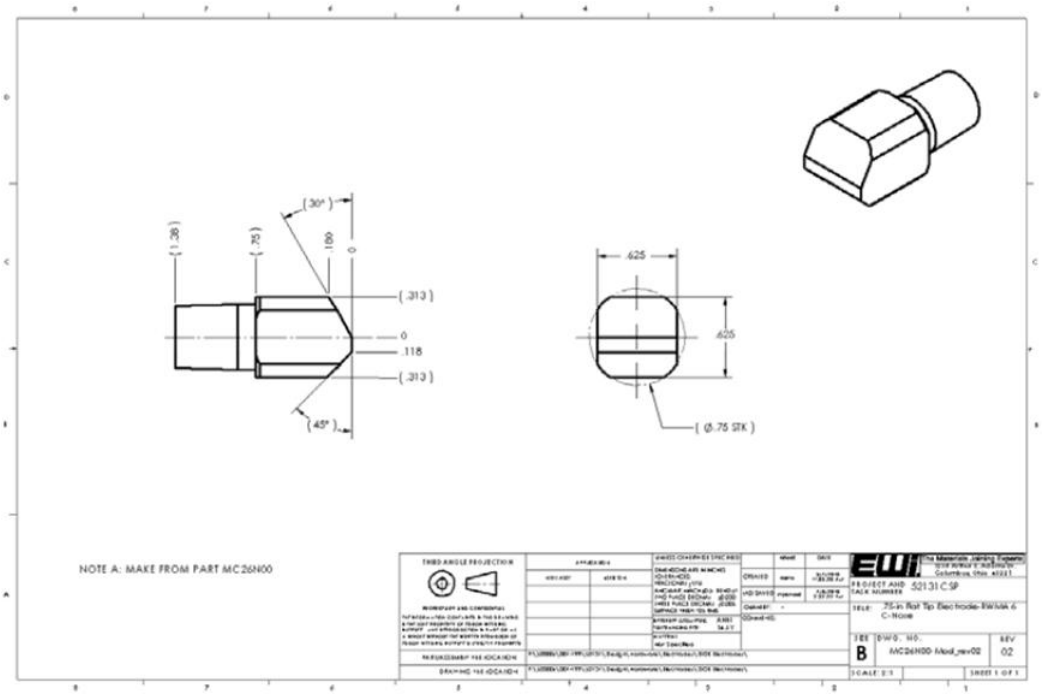

Figure 6. **Square Electrode with both 30- and 45-Degree Angles used on Parallel-Wire Joint Geometry**

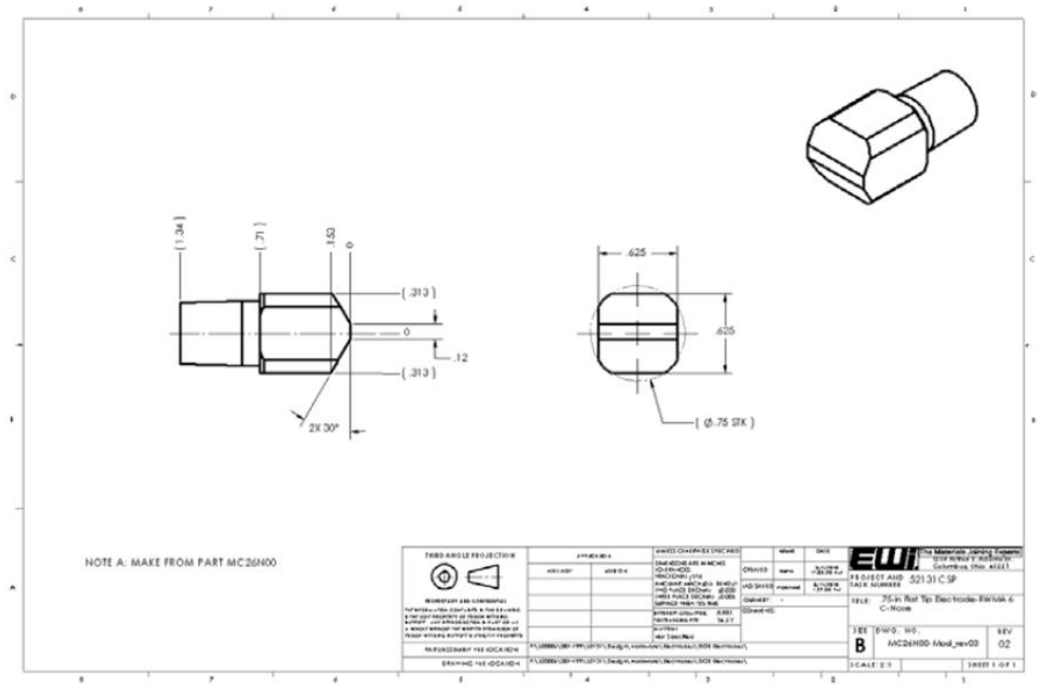

Figure 7. Improved Square Electrode with 30-Degree Angles used on Parallel-Wire Joint Geometry

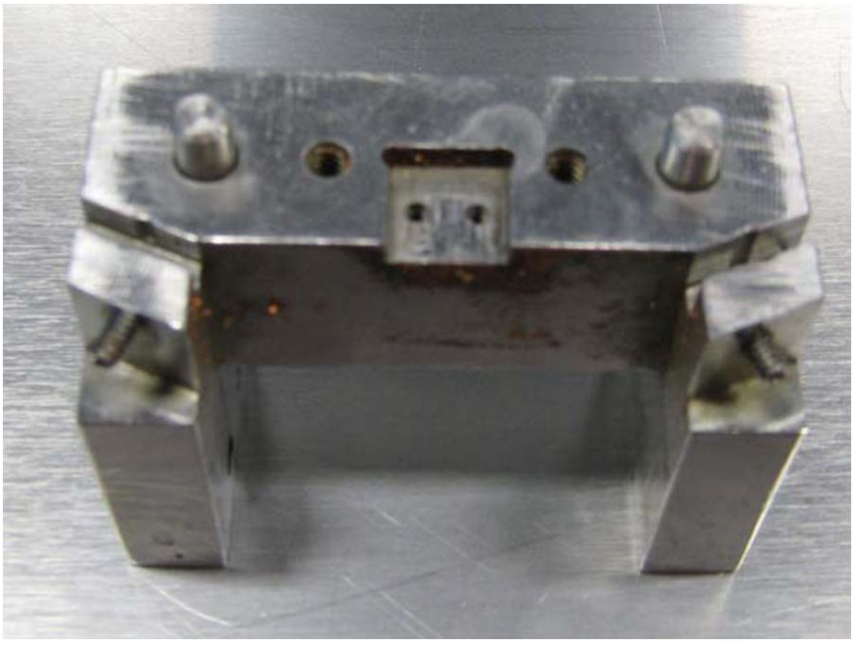

Figure 8. Weld Fixture used for both Cross- and Parallel-Wire Joint Geometries

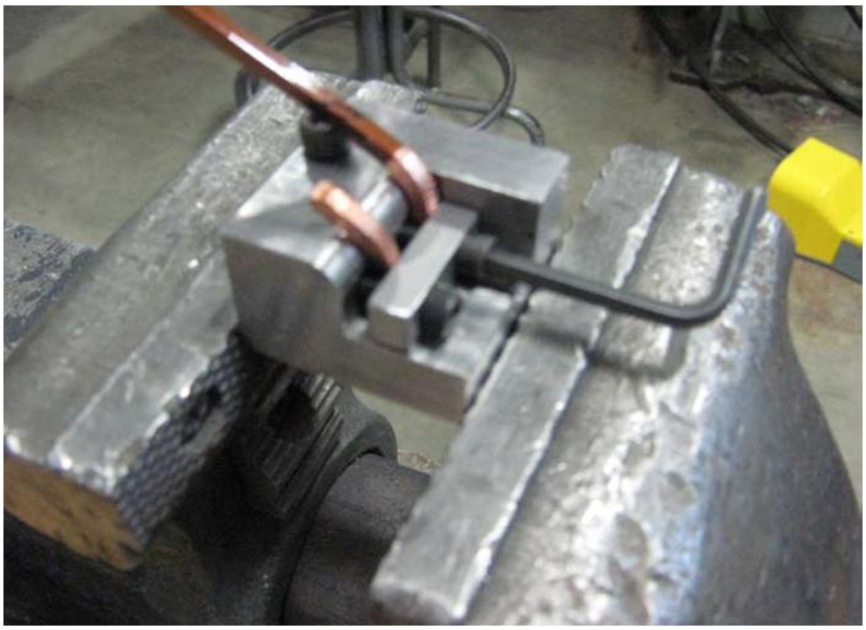

Figure 9. Bend Fixture used to Bend the Wires for the Parallel-Wire Geometry to Nominally a 115-Degree Angle

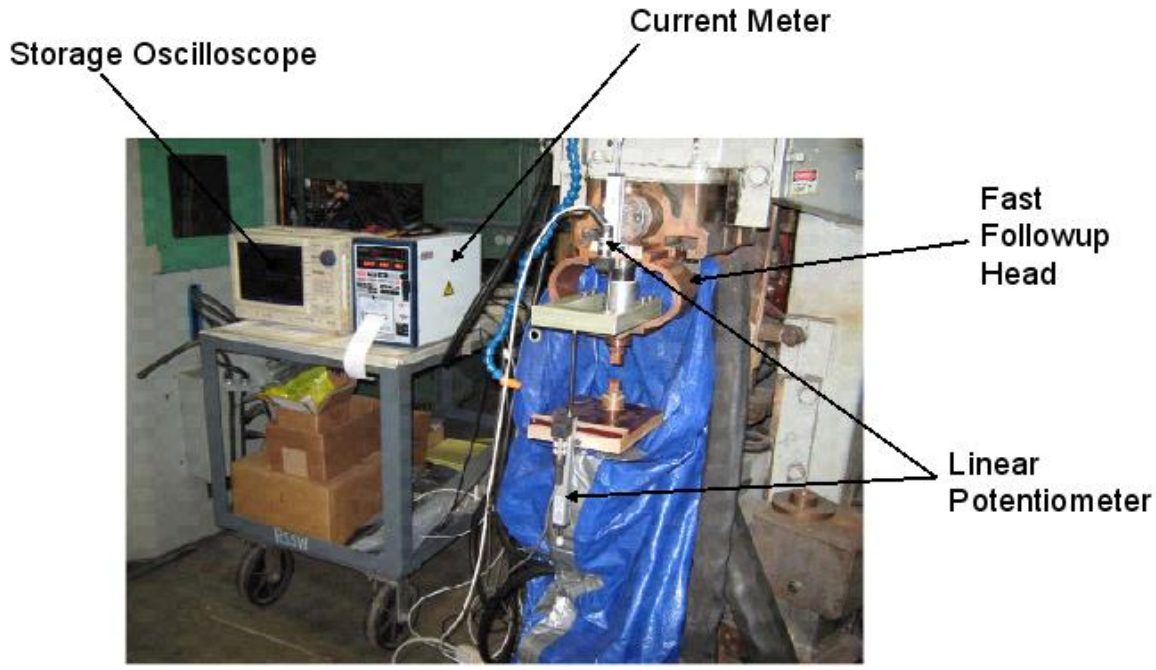

Figure 10. Photograph Showing Data Acquisition Setup

Figure 11. Weld Sample Prepared for Tensile Testing (Parallel-Wire Geometry Shown)

Figure 12. Photograph of Scarred Center Post used to Align the Belleville Washers in the Fast Follow-Up Head (Scarred surface prevented the head from providing follow-up action.)

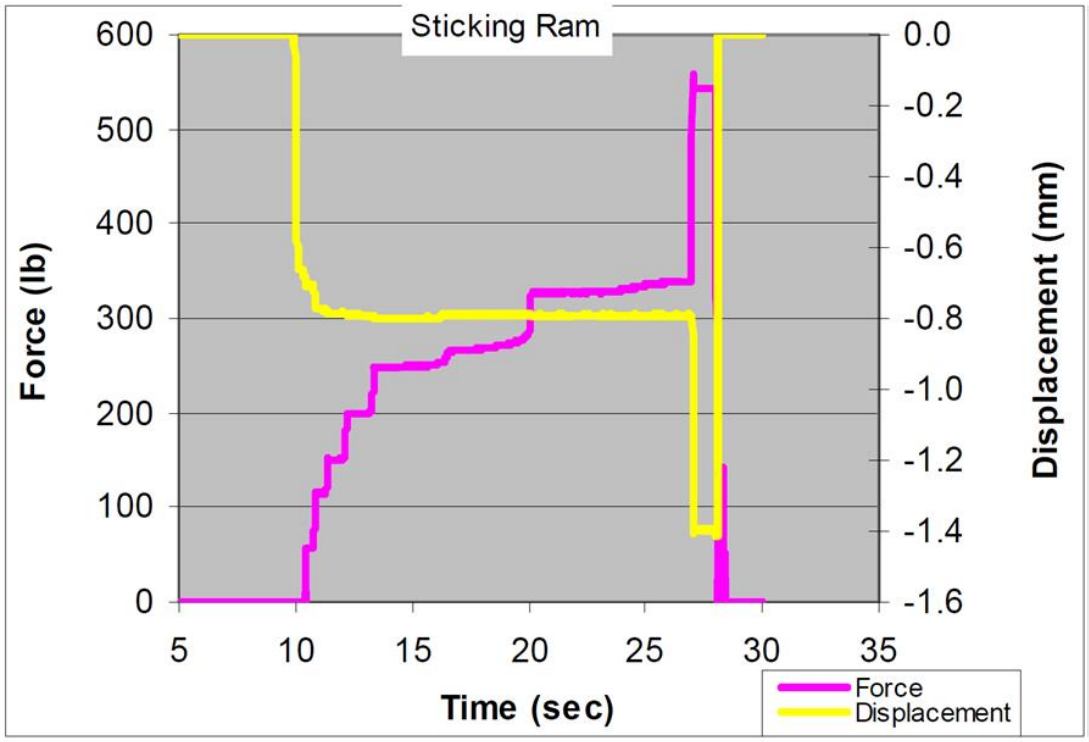

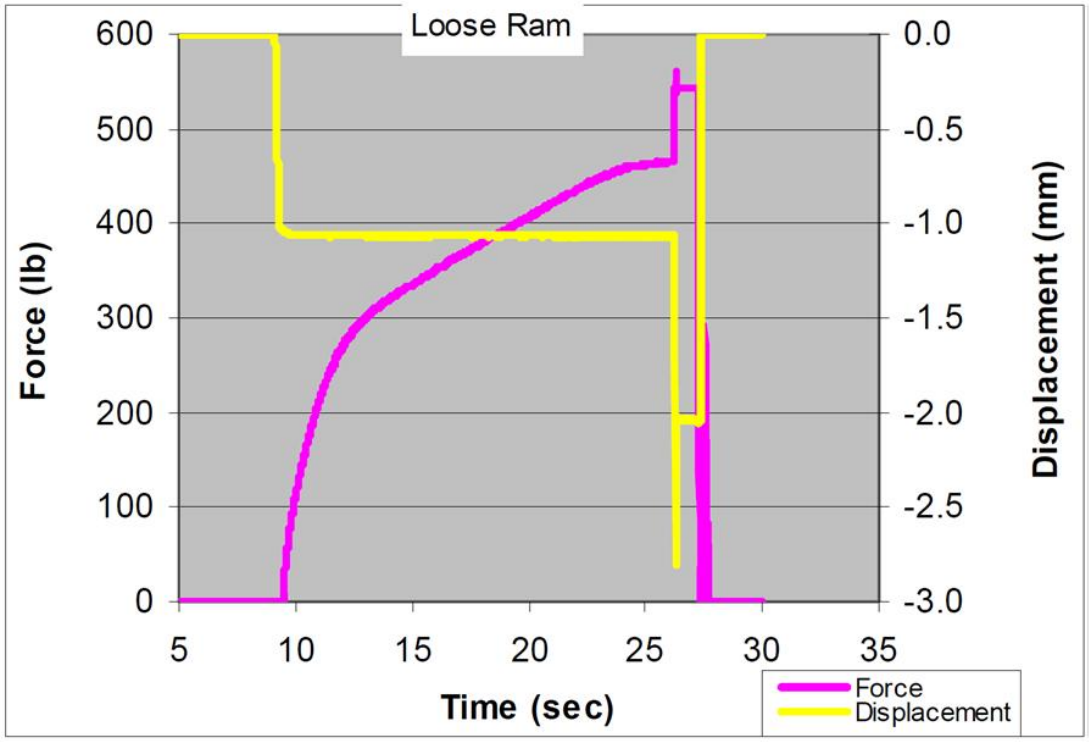

Figure 13. **Plots of Weld Force vs. time Showing Effects of Stiction on Head Motion Caused by Excessive Constraint from the Ram guide** (Upper plot shows head motion with stiction. Lower plot shows head motion without stiction.)

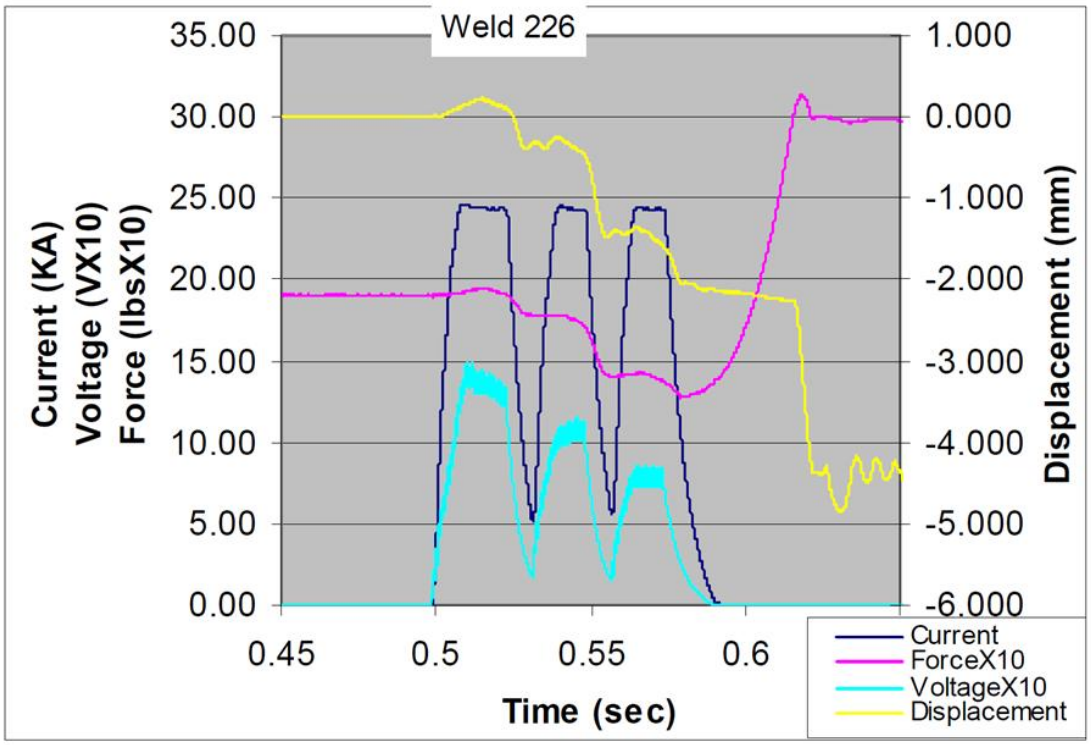

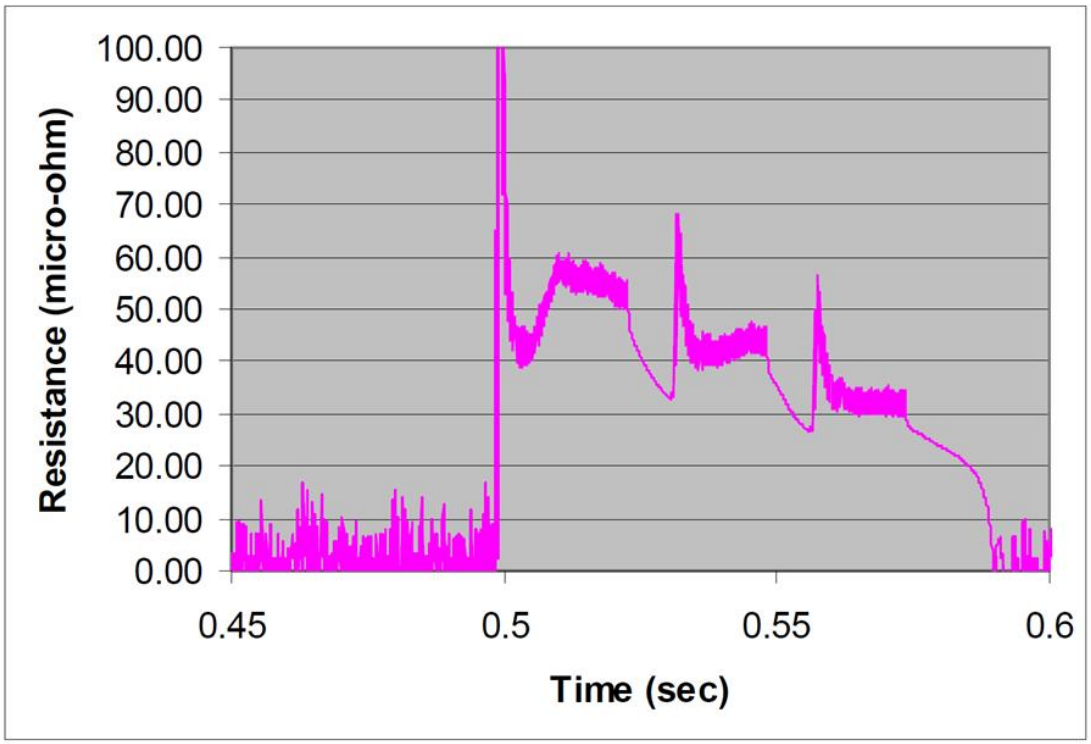

Figure 14. Dynamic Voltage, Current, Force (Measured from Displacement within the Fast Follow-Up Head), and Dynamic Resistance for Weld 226 Representing the Recommended Parameters for the Parallel-Wire Joint Geometry

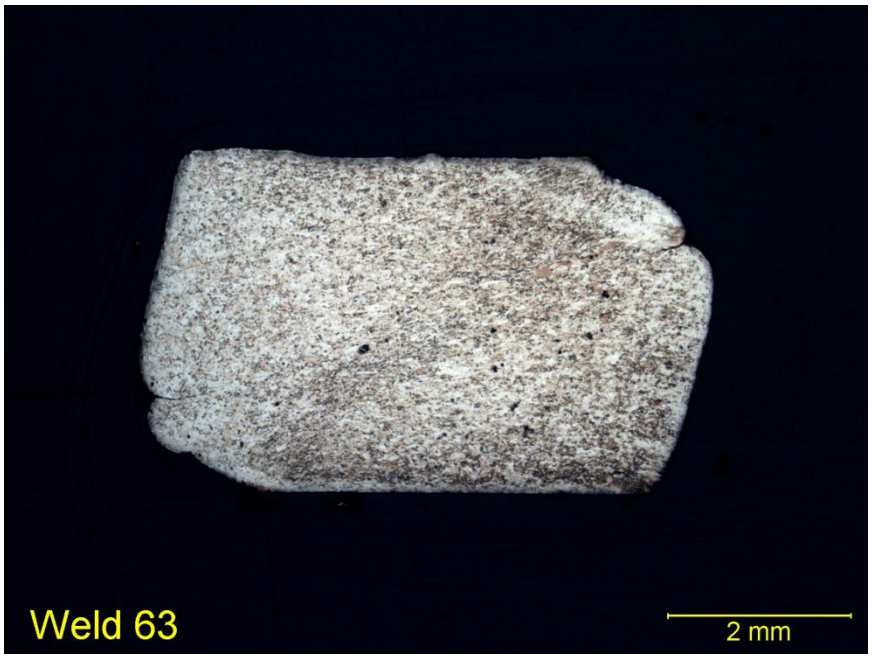

Figure 15. **Micrograph of Weld 63 Showing bond and Microstructure of Cross-Wire Joint using Best-Practice Welding Parameters** (The section was cut transverse to the wire cross direction.)

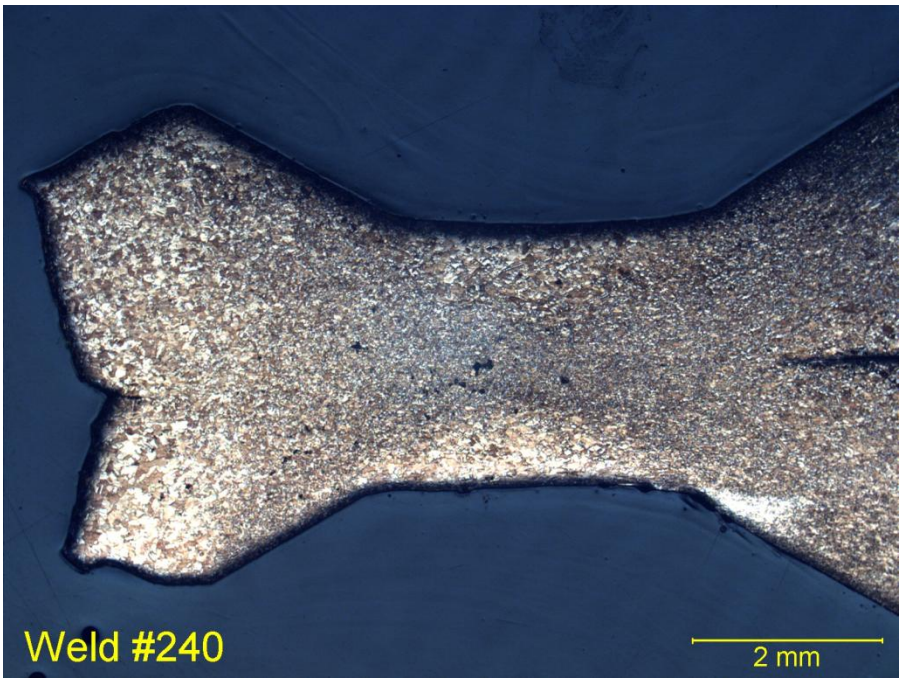

Figure 16. **Micrograph of Weld 240 showing Bond and Microstructure of Parallel-Wire Joint using Best-Practice Welding Parameter (**The section was cut parallel to the wire orientation.)

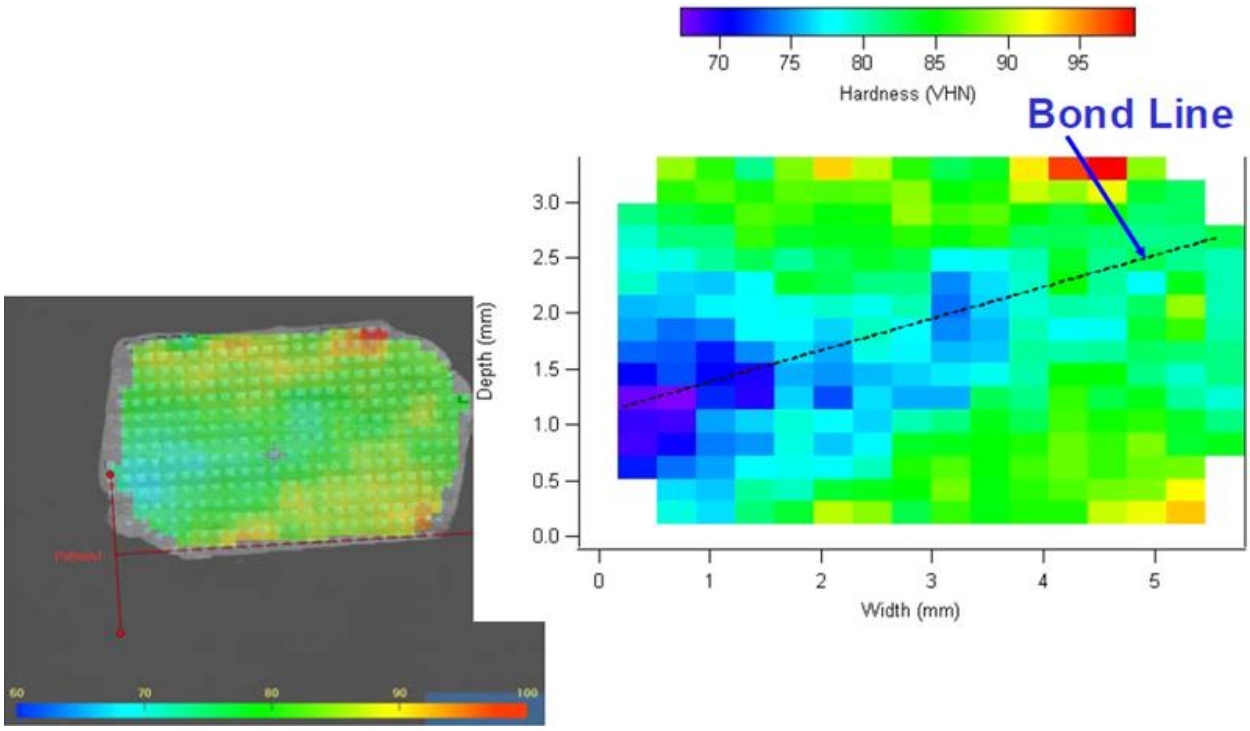

Figure 17. Microhardness of Cross-Wire Weld (Weld 62) for Weld Cross Section

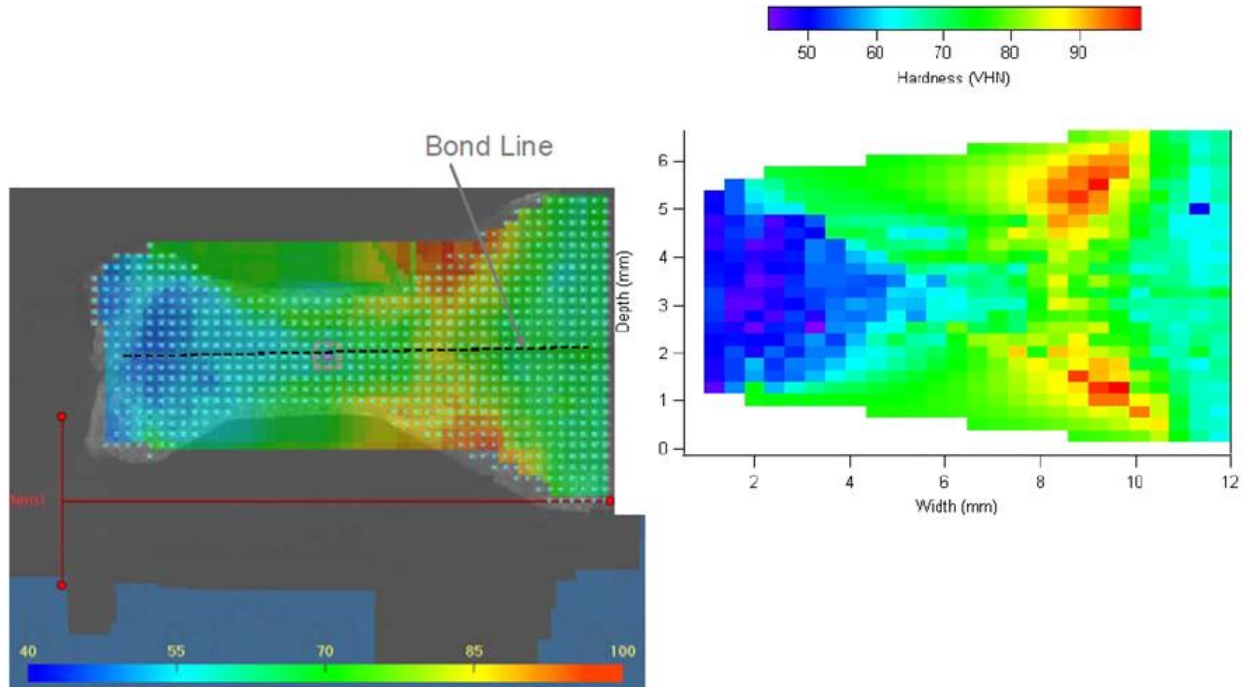

Figure 18. Microhardness of Parallel-Wire Weld (Weld 240) for Weld Cross Section Shown in Figure 12

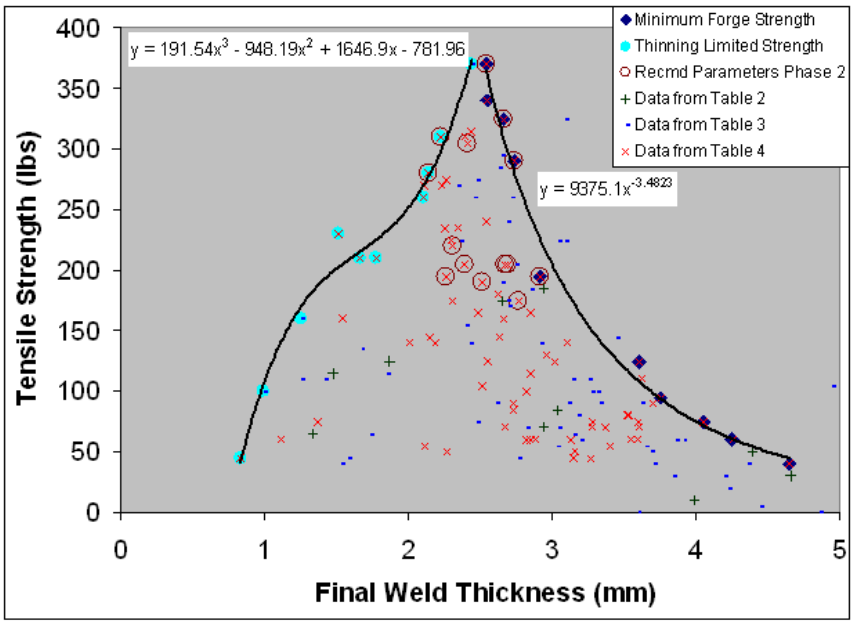

Figure 19. **Summary of Weld Tensile Strength as a Function of final Weld Thickness for the Welds Shown in Tables 2-4** (Upper bounds represent maximum strength under minimal forging conditions and strength loss due to excessive thinning of the wire.)

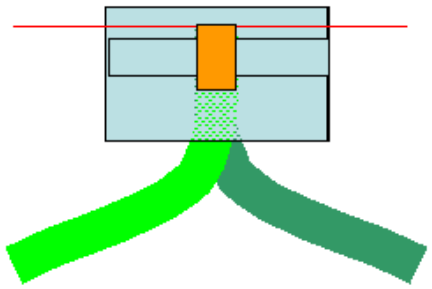

Standard Position:
Heat trapped in free end.
Free end provides constraint to collapse.
Joint heats and softens during weld pulses.
Most heat flows out through bent wires.
Joint collapse is moderate during forging.
Strong weld – lots of strain to bond

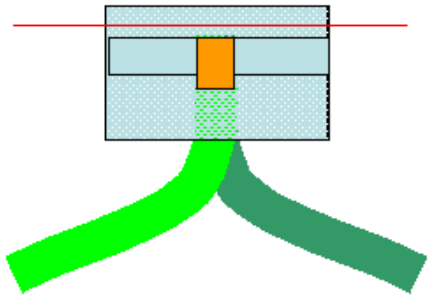

No Extension:
No heat flows out through free end.
No constraint to collapse.
Joint heats and softens during weld impulses.
All heat flows out through bent wires.
Joint collapse is significant during forging.
Strong weld – lots of strain to bond.

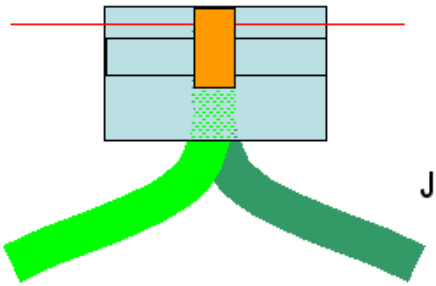

Long Extension:
Heat flows out free end & bent wires..
Free end provides constraint to collapse.
Joint heats, but softens less during weld pulses.
Joint collapse is minimal during forging.
Weak weld - little strain to promote bonding

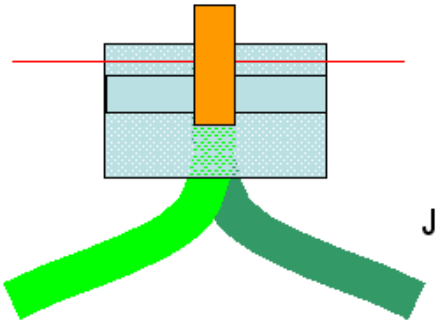

Very Long Extension:
Heat flows out free end & bent wires..
Free end provides constraint to collapse.
Joint heats, but softens less during weld pulses.
Joint collapse is minimal during forging.
Weak weld - little strain to promote bonding

Figure 20. **Schematic Diagram showing the Effect of Heat Flow from the Weld Joint due to Variation in Wire Extension Past the Electrode Edge** (This factor had significant effect on weld strength variability.)